# Interacting Anyons in a One-Dimensional Optical Lattice

**Diplomarbeit in Biophysik**

durchgeführt von

Martin Bonkhoff

am Fachbereich Physik der TU Kaiserslautern

unter Anleitung von

Prof. Dr. Sebastian Eggert

Dezember 2016

# Zusammenfassung

In dieser Arbeit werden die grundlegenden Eigenschaften des eindimensionalen Anyon-Hubbard Modells untersucht, dass, unter Zuhilfenahme einer verallgemeinerten Jordan-Wigner Transformation [1], auf ein Bose-Hubbard Modell mit Dichte-abhängiger Peierls Phase abgebildet werden kann. Zuerst nutzen wir dafür den sogenannten Gutzwiller Molekularfeld-Ansatz aus Ref. [2] und erweitern diesen auf eine verallgemeinerte Form, um sowohl bosonische als auch anyonische Paar-Korrelationsfunktionen zu berechnen. Anschließend werden die korrespondierenden Quasi-Impulsverteilungen diskutiert, welche die aus der Paritätsverletzung resultierende anyonische Vertauschungsstatistik widerspiegeln. Des Weiteren wird die Grenze zwischen suprafluider und isolierender Phase in Abhängigkeit des statistischen Parameters untersucht. Die resultierenden Ergebnisse stehen dabei im Einklang mit denen aus Ref. [1]. Unsere Untersuchungen haben dabei gezeigt, dass die langreichweitige suprafluide Kohärenz durch die statistische Wechselwirkung zerstört wird.

# Abstract

We analyze in detail the properties of the one-dimensional Anyon-Hubbard model, which can be mapped to a corresponding Bose-Hubbard model with a density-dependent Peierls phase via a generalized Jordan-Wigner transformation [1]. At first we extend the modified version of the classical Gutzwiller-mean-field ansatz of Ref. [2] in order to obtain the pair-correlation function for both the bosonic and the anyonic system. With this we discuss how the resulting quasi-momentum distributions reveal in general a parity breaking, which is due anyonic statistics. Afterwards, we determine how the boundary of the superfluid-Mott quantum phase transition changes with the statistical parameter. We find according to Ref. [1] that the statistical interaction has the tendency to destroy superfluid coherence.

# Contents

# 1 Introduction

In the first chapter of the thesis the concept of anyons is introduced on principle. We discuss the topological properties of the configuration space of classical as well as quantum particles, with emphasis on the effects on the fundamental group introduced by the indistinguishabillity of particles. Furthermore two historically important proposals of a generalized exclusion principle are reviewed, in order to differentiate between the concept of exchange statistics and exclusion behavior.

## 1.1 Physical Motivation

Among the most interesting quantum phenomena are those which do not posses any classical analog and, thus are so counterintuitive to the human view of the world, which is indubitably based on classical physics. One of the most fundamental quantum mechanical concept is the indistinguishability of particles accompanied by their exchange statistics, as well as their particle specific algebraic relations. According to the spin-statistics theorem of Wolfgang Pauli [3], only two kinds of elementary particles exist in a space-time of dimension four or higher. One can distinguish them by the response of their wave function under a permutation of their spatial indices.
While the total wave function of particles with an half-integer spin is antisymmetric under a permutation of them, the ones with integer spin stays symmetric under exchange. This fact has some remarkable consequences on the collective behavior of the particles. In the case of bosons, i.e. particles with integer spin, there is no restriction on the occupation of a given state, which is defined by a set of quantum numbers. In contrast to that for fermions, i.e. particles with half-integer spin, there is the Pauli blockade, which means that for a given set of quantum numbers only one particle can occupy such a state. One of the crucial points of the spin-statistics theorem is its restricted validity concerning the dimension of the underlying space-time. That means that in two spatial dimensions or below there could possibly exist other types of particles, which obey other kinds of statistics than those predicted by the spin-statistics theorem.
More precisely, via an exchange of the particles they can acquire a phase, which is different from the extremal ones in a space-time of dimension of at least four. As the phase can take arbitrary many values along the unit circle, one can have an infinite number of statistics, or "any" statistics, which is subsumed under the superordinate concept of anyons [4, 5].
Naively speaking there is no need in dealing with such kind of particles, because our physical world obviously consists of three spatial dimension, but nevertheless there are many examples, primarily in condensed matter physics, of dimensionally reduced systems, which can effectively be described with one- or two-dimensional models. So even these particles may not exist as localized objects, they might be valuable in the sense of a quasi-particle picture describing elementary excitations in low-dimensional systems [6].

Especially the research field of ultra cold atoms should be emphasized in that context, as it represents a playground for studying physical phenomena with a very high degree of controllability. Additionally various kinds of systems can be engineered or simulated which otherwise are not experimentally feasible or even non-existing in nature. Thus, there already exist different proposals for the experimental realization of anyons, or anyon-like systems in different setups [7–10].
Finally, since the last three decades there has been an uprising interest in the interplay between topology and physics, for example topological superconductors [11], or phase transitions driven by topological defects [12]. As anyons are deeply related to the topological properties of the configuration space of particles, the study of their specific properties will definitely contribute to that fascinating interplay of elementary mathematics and physics. Also the application of anyons in realizing topological quantum computation and with that novel non-classical error-corrections as well as algorithms, shall not be forgotten to be mentioned [13].

## 1.2 Topological Background

In this section we will discuss the topology of the configuration space of quantum particles, in comparison to the classical case [5].

The principle of quantum statistics is deeply rooted in the concept of indistinguishability of particles. Usually it is defined by the phase the total wave function of the system picks up, when its constituents are interchanged, i.e. permuted. For instance, in case of a two-particle wave-function we have

$$|\,\Psi\,(x_1, x_2)\,\rangle = \exp(i\theta)|\,\Psi\,(x_2, x_1)\,\rangle. \tag{1.1}$$

The indices labeling the degrees of freedom of the system are not related to physical observables, and a permutation of them leads obviously to the same physical state. Whereas a permutation of indistinguishable objects, in particular the particle operators themselves doesn't make any physical sense. So instead of thinking of a permutation of particles, one should think of a permutation of the index set labeling them. In order to study the exchange statistics in detail, it is necessary to consider the topological properties of the underlying configuration space of identical particles. In a classical system containing $N$ particles, the single particle configuration space of particle $i$ is denoted by $X_i$. Now the whole configuration space is given by the $N$-fold Cartesian product of the single particle space, namely $X_i^N$. This stems from the fact that in classical mechanics point particles are distinguishable, which means that a permutation of them leads to a different physical system. In a quantum mechanical system the situation changes drastically, because every permutation of the constituents of the configuration space leads to the same observables. Thus the true configuration space is correctly defined to be the quotient space $X_i^N/S_N$, with $S_N$ denoting the symmetric group of $N$ letters. As $S_N$ being a finite, discrete and non-abelian group for $N > 2$, the quotient space $X_i^N/S_N$ is locally diffeomorphic to $X_i^N$, except at the points where different particle positions coincide. This set of points is defined as

$$\Delta_N = \big[\{x_i\} \in X_i^N \quad | \quad x_i = x_j \quad \text{for any} \quad i \neq j\big] \tag{1.2}$$

and is excluded for convenience in the following discussion. As the two spaces $\left(X_i^N \setminus \Delta_N\right)$ and $\left(X_i^N \setminus \Delta_N\right)/S_N$ are only locally diffeomorphic, the topological properties can still be different as they depend on their global structure.
In order to reveal the topological structure of $\left(X_i^N \setminus \Delta_N\right)/S_N$ it is assumed that the single particle configuration space $X_i$ coincides with the $d$-dimensional Euclidian space $\mathbb{R}^d$ and for simplicity the focus of the present discussion is on the two-particle case $N = 2$. That means that the space is defined by $\left(\left(\mathbb{R}^d \times \mathbb{R}^d\right) \setminus \Delta_2\right)/S_2$, whereas the set of coincident points, as well as the obsolet permutations can be properly formalized by using relative and center-of-mass coordinates

$$x_{c.m.} = \frac{x_1 + x_2}{2}, \tag{1.3}$$

$$x_r = x_2 - x_1. \tag{1.4}$$

That means we could identify concretely

$$\begin{aligned} \Delta_2 &= \left[x_r \in X_i^2 \quad | \quad x_r = 0 \quad \right], \\ S_2 &= \left[\left(x_{c.m}, x_r\right), \left(x_{c.m}, -x_r\right)\right]. \end{aligned} \tag{1.5}$$

Thus the configuration space is given by,

$$\left(\left(\mathbb{R}^d \times \mathbb{R}^d\right) \setminus \Delta_2\right)/S_2 = \mathbb{R}^d \times \left(S^{d-1}/S_2\right) \times (0, +\infty) \tag{1.6}$$

where $\left(S^{d-1}/S_2\right)$ can be identified with the real projective space $\mathbb{R}P^{d-1}$, i.e. the topological space of lines passing through the origin 0 in $\mathbb{R}^d$. In order to find the topological properties of the configuration space, one needs to compute its fundamental group $\Pi_1$, which gives information about continuous deformations of connecting paths which start and end at a fixed base point. For a mathematically more precise definition one should consult the literature [14, 15]. For the following computation of the fundamental group one can use the fact that $\Pi_1$ of a Cartesian product of two topological spaces, lets say $X$ and $Y$, is equivalent to the direct product of the corresponding two fundamental groups, namely

$$\Pi_1\left(X \times Y\right) = \Pi_1\left(X\right) \bigotimes \Pi_1\left(Y\right). \tag{1.7}$$

Thus it follows

$$\begin{aligned} \Pi_1\left(\mathbb{R}^d \times \left(S^{d-1}/S_2\right) \times (0, +\infty)\right) =& \Pi_1\left(\mathbb{R}^d\right) \bigotimes \Pi_1\left(S^{d-1}/S_2\right) \bigotimes \Pi_1\left((0, +\infty)\right) \\ =& \Pi_1\left(S^{d-1}/S_2\right). \end{aligned} \tag{1.8}$$

This result stems from the fact that both $\mathbb{R}^d$ as well as $(0, +\infty)$ are simply connected topological spaces, which implies a trivial fundamental group, i.e. $\left(\Pi_1\left(\mathbb{R}^d\right) = id = \Pi_1\left((0, +\infty)\right)\right)$, as every path between two points can be continuously deformed into any other such path, while preserving the endpoints. Indeed, every loop in these spaces can be continuously deformed to a

single point and thus they do not posses any holes.
Now one can easily obtain the fundamental group of the real projective space $\mathbb{R}P^{d-1}$ by observing that $\mathbb{R}P^{d-1}$ is the quotient of $S^{d-1}$ by the action of the cyclic group of order 2, i.e. $\mathbb{Z}_2 \cong S_2$. Where $\mathbb{Z}_2$ maps each point on $S^{d-1}$ to its antipode, i.e. sending an $x \in S^{d-1}$ to $-x \in S^{d-1}$.
$\mathbb{Z}_2$ acts freely on $S^{d-1}$, that means for every $x \in S^{d-1}$ and $g \in \mathbb{Z}_2$ the only solution to the equation $gx = x$ is the trivial solution $g = 1$.
Hence one can show that $\pi : S^{d-1} \longrightarrow S^{d-1}/\mathbb{Z}_2 \cong \mathbb{R}P^{d-1}$ is a covering map. That means that for all $x \in S^{d-1}$ there is an open neighborhood $N_x$ such that $\pi^{-1}(N_x)$ is a disjoint union of open sets, each of which is mapped homeomorphically by $\pi$ onto $N_x$. So one can conclude, as $S^{d-1}$ is connected, path-connected and locally path-connected for $d - 1 > 1$, that $\Pi_1\left(\mathbb{R}P^{d-1}\right)/\Pi_1\left(S^{d-1}\right) \cong \mathbb{Z}_2$ and therefore $\Pi_1\left(\mathbb{R}P^{d-1}\right) \cong \mathbb{Z}_2$. While on the other hand $\Pi_1\left(\mathbb{R}P^1\right) \cong \mathbb{Z}$.

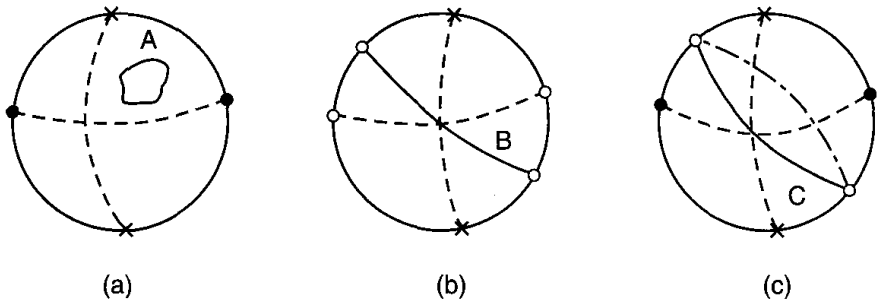


**FIG. 1.1:** All closed paths in the configuration space in $d \geq 3$ [5]. a) no exchange and thus contractible, b) single exchange to diametrically opposite points and thus non-contractible, c) two consecutive exchanges forming a contractible loop

That can be explained as follows, if $d \geq 3$ the space $S^{d-1}$ is simply connected and thus it is the universal covering space of $\mathbb{R}P^{d-1}$, i.e. $S^{d-1}$ covers any connected cover of $\mathbb{R}P^{d-1}$. Thus the fundamental group of $\mathbb{R}P^{d-1}$ is given by $\Pi_1\left(\mathbb{R}P^{d-1}\right) = \mathbb{Z}_2$.
In the case that $d = 2$, however $\mathbb{R}P^1$ is homeomorphic to $S^1$, where $S^1$ is universally covered by $\mathbb{R}$. Thus it follows that $\Pi_1\left(S^1\right)/\Pi_1(\mathbb{R}) \cong \mathbb{Z} = \Pi_1\left(\mathbb{R}P^1\right)$, where $\mathbb{Z}$ denotes the infinite cyclic group.

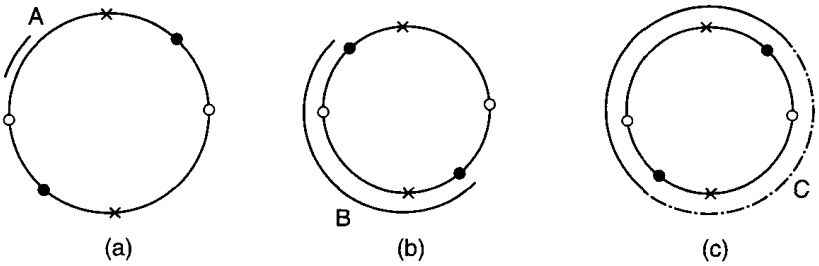


**FIG. 1.2:** All possible closed paths in the two-dimensional configuration space [5]. a) no exchange, b) single non-contractible exchange as the endpoints are fixed, c) two consecutive exchanges forming a non-contractible loop

In one spatial dimension $d = 1$, the configuration space consists of a single point $\mathbb{R}P^0$ and thus its fundamental group is trivial $\Pi_1\left(\mathbb{R}P^0\right) = id$.
Note that it is difficult to define quantum statistics in one dimension, as the particles can not exchange without passing through each other and thus statistics is inextricably interwined with local interactions. The explicit calculation of the general $N$-particle case was done in [16, 17] and yields the fundamental result,

$$\Pi_1\left(((\mathbb{R}^d)^N \setminus \Delta)/S_N\right) = id \ ; \ \text{for} \ d = 1, \tag{1.9}$$

$$\Pi_1\left(((\mathbb{R}^d)^N \setminus \Delta)/S_N\right) = B_N \ ; \ \text{for} \ d = 2, \tag{1.10}$$

$$\Pi_1\left(((\mathbb{R}^d)^N \setminus \Delta)/S_N\right) = S_N \ ; \ \text{for} \ d \geq 3, \tag{1.11}$$

where $B_N$ stands for the Braid group of $N$-strands. In the case of $S_N$ there are only two one-dimensional, unitary, irreducible representations, namely the trivial and the alternating one which correspond to bosons or fermions, respectively, while higher-dimensional representations correspond to parastatistics [5]. Whereas in the case of $B_N$, being an infinite group, there is a continuous family of one-dimensional representations which correspond to different abelian anyons, as well as higher-dimensional representations, which correspond to non-abelian anyons. At this point the careful reader should be confused by the fact, that strictly speaking anyons are only realized in two spatial dimension, while the title of the thesis implies that it is about their occurrence in a one-dimensional setting. However the discussion of that putative contradiction is displaced to a later chapter, where the connection between anyons in one dimension to their two-dimensional counterpart will be explained by means of their algebraic properties.

## 1.3 Exclusion Principle

In the following part we will review exemplarily two historically important generalizations of the Pauli exclusion principle, where it should be noted that there exist many different proposals to interpolate between bosonic and fermionic exclusion behavior [5]. In order to relate the plethora of different proposals one can compare the Virial expansion of an ideal gas of particles obeying these statistics with the anyonic case [5]. It turns out that none of these proposals coincide among each other, nor with the anyonic case [18]. The crucial point is that the exchange statistics depends on the spatial dimension of the configuration space, which is manifested in the algebraic relations for the non-local (anti)–commutators, connecting different sites of the lattice. In contrast to that the exclusion behavior, which determines how many particles can occupy a certain state, is related to the local (anti)–commutator relations that connect operators on a single lattice site. By an explanation of the algebraic relations of the different proposals, the difference between them and the anyonic commutation relation that will be introduced in the next chapter is pointed out on a fundamental level. The discussion is based on Ref. [19].

### 1.3.1 Haldane Exclusion Principle

We start with a possible second-quantized realization of the generalized exclusion principle suggested by Haldane [20]. As the exclusion behavior is dictated by the local commutation relations, it is sufficient to restrict the discussion to the following single mode algebra, for creation and annihilation operators $\hat{g}^\dagger$ and $\hat{g}$

$$\begin{aligned} \left[\hat{g}, \hat{g}^\dagger\right] &= 1 - \hat{F}\,, \\ \left[\hat{g}^\dagger, \hat{g}^\dagger\right] &= 0\,, \\ [\hat{g}, \hat{g}] &= 0\,, \\ \left[\hat{g}^\dagger \hat{g}, \hat{g}^\dagger\right] &= \hat{g}^\dagger\,, \end{aligned} \tag{1.12}$$

where $\hat{F} = \hat{F}^\dagger$ is a polynomial in $\left(\hat{g}^\dagger, \hat{g}\right)$ such that $\hat{g}^\dagger \hat{F} = 0$. A possible choice for the polynomial is $\hat{F} = \left(\hat{g}^\dagger\right)^p (\hat{g})^p$, where $p$ is an arbitrary integer with $p > 0$. The algebra (1.12) corresponds to a certain deformation of the bosonic Heisenberg algebra, and together with $\hat{F} = \left(\hat{g}^\dagger\right)^p (\hat{g})^p$, is one out of infinitely many realizations of a fractional exclusion algebra for the same value of $p$. One can show that the presence of $\hat{F}$ in the deformed commutation relation leads to the following nilpotency condition for that kind of particles $\left(\hat{g}^\dagger\right)^{p+1} = 0$, thus the dimension of the local Hilbert space is restricted to $p + 1$. In comparison, fermions would correspond to $p = 1$, while for bosons $p$ can be any integer larger than 1.

### 1.3.2 Green Exclusion Principle

The next example is the algebra of para-particles, which was first introduced by Green [21]. The idea is to introduce auxiliary modes, labeled by the Green indices $\alpha = 1, ..., p$ for the usual $CCR$, or $CAR$. Where $CCR\,(CAR)$ stands for canonical (anti)-commutation relations.

$$\left[\hat{d}_{i,\alpha}, \hat{d}^\dagger_{j,\alpha}\right]_k = \delta_{i,j} \hat{I} \tag{1.13}$$

$$\left[\hat{d}_{i,\alpha}, \hat{d}_{j,\alpha}\right]_k = 0 = \left[\hat{d}^\dagger_{i,\alpha}, \hat{d}^\dagger_{j,\alpha}\right]_k \tag{1.14}$$

where $k = \mp 1$ correspond to fermions or bosons respectively. Now for different Green indices $\alpha \neq \beta$, the following relations are introduced,

$$\left[\hat{d}_{i,\alpha}, \hat{d}^\dagger_{j,\beta}\right]_{-k} = 0 \tag{1.15}$$

$$\left[\hat{d}_{i,\alpha}, \hat{d}_{j,\beta}\right]_{-k} = 0 = \left[\hat{d}^\dagger_{i,\alpha}, \hat{d}^\dagger_{j,\beta}\right]_{-k}. \tag{1.16}$$

Para-bosons, or para-fermions are now defined as a sum over all these artificial modes,

$$\hat{c}^\dagger_i = \sum_{\alpha=1}^{p} \hat{d}^\dagger_{i,\alpha}, \tag{1.17}$$

$$\hat{c}_i = \sum_{\alpha=1}^{p} \hat{d}_{i,\alpha}, \tag{1.18}$$

which satisfy the following relations,

$$\left[\left[\hat{c}_i^\dagger, \hat{c}_j\right]_{-k}, \hat{c}_l\right]_{k=1} = -2\delta_{i,l}\hat{c}_j, \tag{1.19}$$

$$\left[\left[\hat{c}_i, \hat{c}_j\right]_{-k}, \hat{c}_l\right]_{k=1} = 0. \tag{1.20}$$

Additionally one can define a set of number operators via

$$\hat{n}_j = \frac{1}{2}\left(\left[\hat{c}_i^\dagger, \hat{c}_i\right]_{-k} \pm p\right) = \sum_{\alpha=1}^{p} \hat{d}_{i,\alpha}^\dagger \hat{d}_{i,\alpha}. \tag{1.21}$$

Now, in the case of fermions every mode is subject to the Pauli principle, thus $\left(\hat{d}_{i,\alpha}^\dagger \hat{d}_{i,\alpha}\right)^2 = \hat{d}_{i,\alpha}^\dagger \hat{d}_{i,\alpha}$. That implies that para-fermion number operator $\hat{n}_j$ has eigenvalues in the interval $[0, p]$. Furthermore, the following relation holds.

$$\left(\hat{c}_i^\dagger\right)^p = p! \prod_{\alpha=1}^{p} \hat{d}_{i,\alpha}^\dagger \tag{1.22}$$

Thus $\left(\hat{c}_i^\dagger\right)^{p+1} = 0$, which can also be interpreted as a generalized Pauli principle. From that point of view canonical bosons (fermions) are para-bosons (para-fermions) of order $p = 1$.

## 1.4 Outline of the Thesis

After having provided both the physical and the topological background of anyonic physics, the second chapter works out the notion of one-dimensional anyons in optical lattices by the example of the Anyon-Hubbard model. Additionally a special kind of Jordan-Wigner transformation is represented, in order to relate one-dimensional anyons with ordinary bosons [1]. The algebraic structure of these Jordan-Wigner anyons is discussed in detail, and compared to the one of the standard anyonic commutation relations. Via this transformation it is possible to map the Anyon-Hubbard model to a bosonic model with density-dependent Peierls phase. Furthermore three different experimental proposals to realize that bosonic model with correlated hopping in a optical lattice are reviewed and compared [1, 22, 23].

In the third chapter we analyze the classical symmetries of the bosonic model for different boundary conditions in detail, as the effect of the chosen boundary conditions is widely neglected in the literature. The focus is made especially on space-time symmetries, as parity and time-reversal violations are inherent to anyonic systems [5]. The generators, which mediate these spatial transformations, are constructed explicitly by elementary bosonic transposition operators [24, 25]. Furthermore the re-emergence of space-time symmetries for special values of the statistical parameter transmuting between bosonic and fermionic behavior is highlighted.

In the fourth chapter the ground-state properties of the bosonic model is analyzed via the Gutzwiller mean-field approach. In Ref. [2] a modified Gutzwiller ansatz was proposed, where it was claimed that their ansatz is superior to the classical Gutzwiller case. We critically discuss that claim and propose a different ansatz to overcome certain discrepancies. Additionally we

use our ansatz to calculate bosonic as well as anyonic quasi-momentum distribution functions, which are then compared to quasi-exact data obtained by DMRG calculations. The modified ansatz describes the shift of the quasi-momenta due to a breaking of parity or time-reversal symmetry correctly, and is qualitatively in good agreement with the numerical data.

In the fifth chapter we propose a mean-field decoupling ansatz in the spirit of our modified Gutzwiller approach in chapter 4. This decoupling ansatz includes the one of Ref. [1] as a special case. With this we calculate the phase-diagram of the bosonic model. Unluckily we were not able to finish the whole extremalization process in time, thus we always have two possible phase-diagrams, depending on how the phases of the variational parameters are adjusted. Nevertheless it turns out that our approach leads naturally to the presence of a different type of superfluid as discussed in Ref. [26] and if the extremalization would be complete, both transitions could be displayed in contrast to [1][26].

# 2 Anyon-Hubbard Model

In the following chapter we introduce the Anyon-Hubbard of Ref. [1]. One should note that this Hamiltonian does not originate from a microscopic model, but is defined a priori. The reason why one studies this model, is because it is connected to a certain bosonic model via the Jordan-Wigner mapping which will be discussed in the next subsection. Hereafter we discuss different proposals for the experimental implementation of the bosonic model as well as a detailed symmetry analysis of it.

## 2.1 Anyon-Hubbard Hamiltonian

The following model describes the hopping processes of locally interacting anyons in a one dimensional optical lattice, within the tight-binding approximation. The structure of the Hamiltonian is identical to the Bose-Hubbard Hamiltonian [1].

$$\hat{H} = \frac{U}{2} \sum_i \hat{n}_i \left(\hat{n}_i - 1\right) - J \sum_i \left(\hat{a}_i^\dagger \hat{a}_{i+1} + \text{h.c.}\right) - \mu \sum_i \hat{n}_i \tag{2.1}$$

The parameter $U$ scales the on-site interaction, which is repulsive for $U > 0$ and attractive for $U < 0$. The interaction term also possesses a combinatorial interpretation which can be understood by counting the number of possible two-body interactions in an $n$-particle system, disregarding their order. Therefore the model includes local occupation beyond the hard-core limit, which means that the anyonic operators are not subject to any nilpotency condition. Furthermore $J$ determines the strength of the kinetic energy of the particles, which allows them to move from one lattice site to another. The chemical potential $\mu$ denotes the change of energy in the system if particles are added or removed. The index set of the summation index $i$ depends on the chosen boundary conditions of the system. On the level of operators, $\hat{n}_i = \hat{a}_i^\dagger \hat{a}_i$ describes the local occupation of particles at site $i$. Here the anyonic creation and annihilation operators are defined as $\hat{a}_i^\dagger$ and $\hat{a}_i$ and obey a deformed multimode Heisenberg algebra

$$\begin{aligned}\left[\hat{a}_i, \hat{a}_j^\dagger\right]_{q_{i,j}^{\mp}} &= \delta_{i,j}\hat{I}\,,\\ \left[\hat{a}_i^\dagger, \hat{a}_j^\dagger\right]_{q_{i,j}^{\mp}} &= 0\,,\\ \left[\hat{a}_i, \hat{a}_j\right]_{q_{i,j}^{\pm}} &= 0\,,\end{aligned} \tag{2.2}$$

with

$$[A, B]_q = AB - qBA\,, \tag{2.3}$$

$\delta_{i,j}$ being the Kronecker-delta and $\hat{I}$ the identity operator. The deformation is defined as

$$q_{i,j} = \exp\left[\pm i\theta \mathrm{sgn(i-j)}\right]\,, \tag{2.4}$$

where $\mathrm{sgn(i-j)}$ is defined as the Signum function and $\theta \in [0, \pi]$ denotes the statistical parameter. The deformation $q_{i,j}$ obeys the following properties

$$\begin{aligned} q_{i,j} = q_{j,i}^{-1} = q_{j,i}^{*}\,,\\ q_{i,i} = 1 \quad \text{for all} \quad i \in [1, L]\,.\end{aligned} \tag{2.5}$$

The different signs in (2.4) correspond to how the obtained phase is defined, either clockwise or anti-clockwise along the unit circle, depending on the order relation for the spatial coordinates of the particles.
A closer look at the Hamiltonian (2.1) reveals already some interesting properties of one-dimensional anyons. The interaction as well as the chemical potential term are equivalent to its bosonic pendant, which can be interpreted such, that locally anyons behave just as their parent particles out of whom the deformation was defined. More interesting is the kinetic part, where a short calculation shows.

$$\left[-\left(\hat{a}_i^\dagger \hat{a}_{i+1} + \mathrm{h.c.}\right), \hat{a}_i\right]_{q_{i,i+1}} = \hat{a}_{i+1}\exp(-i\theta). \tag{2.6}$$

Thus interchanging two particles and equips them with a phase depending on their spatial order. It should be noted that, except a formal analogy, the deformed commutators in (2.3) have nothing to do with the so called $q$-deformed commutators [27]. This stems from the fact that ordinary $q$-deformations can be defined in any dimension, and are not restricted to one or two dimensions, respectively. Furthermore, ordinary $q$-deformation affects also the local commutators, whereas the anyonic commutators are intrinsically non-local. This can be seen by noticing that one can define a single mode $q$-oscillator, whereas in the case of an anyonic oscillator, would reduce to

the standard bosonic variant.
As a final remark, we want to legitimate the concept of anyons in one spatial dimension, even the configuration space does not inherently posses such a rich structure as in two spatial dimension. It turns out that the deformed commutation relations (2.2), originating from the concept of anyons in two dimensions, can be consistently defined also in one dimension. The stems from the fact that on a one-dimensional line, there is always a natural linear order [28]. Thus commutation relations like (2.2) can be defined a priori, without defining a special point of reference as in the two-dimensional case.

## 2.2 Fractional Jordan-Wigner Transformation

Now we will discuss a generalization of the ordinary Jordan-Wigner-mapping, which was used to demonstrate the equivalence between the one-dimensional Heisenberg-model and a model of spinless fermions with nearest neighbor interaction [29]. The basic idea behind this mapping was that the spin-$\frac{1}{2}$ operators are subject to $CAR$ locally, while the obey $CCR$ non-locally. Exactly this circumstance will also be of importance for the following generalization, especially for the difference between exclusion behavior and exchange statistics.

### 2.2.1 Definition

In order to relate the abstract concept of anyonic statistics to something experimentally feasible, An exact unitary mapping between anyons and particles which succumb the ordinary spin-statistics theorem is introduced [1]. The non-local operators mediating this transformation are defined as follows,

$$\hat{K}_{-,i} = \exp\left(i\theta \sum_{k<i} \hat{n}_k\right) = \prod_{k=1}^{i-1} \exp(i\theta\hat{n}_k), \tag{2.7}$$

$$\hat{K}_{+,i} = \exp\left(i\theta \sum_{l>i} \hat{n}_l\right) = \prod_{l=i+1}^{L} \exp(i\theta\hat{n}_l), \tag{2.8}$$

where the number operator $\hat{n}_i$ can represent bosons, fermions or constrained versions of them. Furthermore the index set contains all sites on the one-dimensional lattice either smaller or larger then the site $i$. In the following discussion we focus on the two standard cases where the parent particles are either canonical bosons or fermions, which obey the usual $CCR$ or $CAR$,

$$\left[\hat{d}_i, \hat{d}_j^\dagger\right]_k = \delta_{i,j}\hat{I} \tag{2.9}$$

$$\left[\hat{d}_i, \hat{d}_j\right]_k = 0 = \left[\hat{d}_i^\dagger, \hat{d}_j^\dagger\right]_k \tag{2.10}$$

$$\hat{n}_i = \hat{d}_i^\dagger \hat{d}_i \tag{2.11}$$

where again $k = \mp 1$ corresponds to fermions or bosons respectively. From the previous definitions it is obvious that the non-local operators (2.7),(2.8) are unitary

$$\hat{K}^{\dagger}_{j,i} = \hat{K}^{-1}_{j,i} \quad \text{for all} \quad j = -, + \tag{2.12}$$

These so called disorder operators act as an identity operation on the creation or annihilation operators on site $i$, whereas they induce a phase shift on the corresponding operators out of the index sets $k$,$l$.

$$\begin{aligned} \hat{K}^{\dagger}_{j,i} \hat{d}_q \hat{K}_{j,i} = \hat{d}_q \exp(i\theta) \\ \forall j = -, + \\ \forall q \in \ k, l \end{aligned} \tag{2.13}$$

Note that the number operator $\hat{n}_i$ is clearly invariant under the action of the Jordan-Wigner string

$$\hat{K}^{\dagger}_{j,i} \hat{n}_q \hat{K}_{j,i} = \hat{n}_q \quad \forall j = -, +; \quad \forall q \in [1, L] \tag{2.14}$$

Additionally these operators mutually commute

$$\left[\hat{K}_{j,i}, \hat{K}_{n,m}\right]_{k=1} = 0 \quad \text{for all} \quad i, j, n, m = -, +, \tag{2.15}$$

Now we can define the anyonic operators in terms of bosons or fermions respectively,

$$\hat{a}_{-,i} = \hat{d}_i \hat{K}_{-,i} \tag{2.16}$$

$$\hat{a}_{+,i} = \hat{d}_i \hat{K}_{+,i}. \tag{2.17}$$

### 2.2.2 Algebraic Properties

In the following,we derive and discuss the algebraic structure of the Jordan-Wigner anyons defined by (2.16)–(2.17). It is similar to a two-particle multimode Heisenberg algebra, but also possesses some unusual algebraic properties.
The operators $[\hat{a}_{l,i}, \hat{a}^{\dagger}_{l,i}, \hat{n}_i, \hat{I}]$ , for all i $\in [1, L]$ and $l = -, +$ span the algebra with classical

commutators and deformed ones as follows

$$\hat{a}_{l,i}\hat{a}_{l,j} - kq_{i,j}^{\pm}\hat{a}_{l,j}\hat{a}_{l,i} = 0, \tag{2.18}$$

$$\hat{a}_{l,i}^{\dagger}\hat{a}_{l,j}^{\dagger} - kq_{i,j}^{\mp}\hat{a}_{l,j}^{\dagger}\hat{a}_{l,i}^{\dagger} = 0, \tag{2.19}$$

$$\hat{a}_{l,i}\hat{a}_{l,j}^{\dagger} - kq_{j,i}^{\mp}\hat{a}_{l,j}^{\dagger}\hat{a}_{l,i} = \delta_{ij}\hat{I}, \tag{2.20}$$

$$\left[\hat{a}_{+,i}, \hat{a}_{-,j}^{\dagger}\right]_k = \delta_{ij} exp\left[i\theta(\sum_{k<i}\hat{n}_k - \sum_{l>j}\hat{n}_l)\right], \tag{2.21}$$

$$\left[\hat{a}_{+,i}, \hat{a}_{-,j}\right]_k = 0, \tag{2.22}$$

$$\left[\hat{a}_{+,i}^{\dagger}, \hat{a}_{-,j}^{\dagger}\right]_k = 0, \tag{2.23}$$

$$\left[\hat{n}_i, \hat{a}_{l,j}^{\dagger}\right]_{k=1} = \delta_{ij}\hat{a}_{l,j}^{\dagger}, \tag{2.24}$$

$$\left[\hat{n}_i, \hat{a}_{l,j}\right]_{k=1} = -\delta_{ij}\hat{a}_{l,j} \tag{2.25}$$

$$\left[\hat{n}_i, \hat{n}_j\right]_{k=1} = 0, \tag{2.26}$$

$$\left[\bullet, \hat{I}\right]_{k=1} = 0. \tag{2.27}$$

Note that the deformation $q_{i,j}^{\pm}$ was already defined in (2.4), with the properties (2.5).

It should be noted that the relations (2.18)–(2.20) are identical to the deformed (anti)-commutation relations (2.2), if one considers the case $k = 1$. They represent the fact that anyons of a given type acquire a phase upon exchange (1.1), which is dependent on the ordering of their spatial indices . At this point it is absolutely crucial to observe, that in the case that $i = j$ the formulas (2.18)–(2.20) reduce to the standard $CCR$ or $CAR$ respectively, which means that the dimension of the local Hilbert space is dictated by the type of parent particles and thus is invariant with respect to the Jordan-Wigner mapping [19]. That shows in a remarkable manner that the exchange statistics and the exclusion principle are two distinct concepts, the former is determined by the non-local (anti)-commutators, whereas the latter is determined by the local ones. That means within this framework it is impossible to transmute from bosons to fermions by a modulation of $\theta$. Nevertheless it is possible, starting from fermions, to transmute into hard-core bosons or, starting from bosons, to pseudo-fermions. Additionally the exchange of two different types of anyons (2.21)–(2.23) is in principle governed by the exchange statistics of their parent particles out of whom they were defined.

Also the algebraic structure of the anyonic commutation relations (2.18)–(2.20) is more complicated as the usual multimode Heisenberg-algebra, and actually admits not even a Lie-algebraic structure in the classical sense. This can be understood by noticing that the anyonic commutators are not a closed bilinear form under all combinations of elements of the algebra, i.e.

$$[\alpha A + \beta B, C]_{q^{\pm}} \neq \alpha\,[A, C]_{q^{\pm}} + \beta\,[B, C]_{q^{\pm}}\,, \tag{2.28}$$

$$[C, \alpha A + \beta B]_{q^{\pm}} \neq \alpha\,[C, A]_{q^{\pm}} + \beta\,[C, B]_{q^{\pm}}\,, \tag{2.29}$$

and thus are not of the classical Lie type. Here the presence of a closed bilinear form depends on the spatial order of the involved elements of the algebra. As an example we calculate

$$[\alpha\hat{a}_i + \beta\hat{a}_l, \hat{a}_k]_{q^{\pm}}\,, \tag{2.30}$$

where we have three spatial indices $i, l, k$. In order to evaluate (2.30) we need to fix a particular order of the index set. After re-insertion of one of the Jordan-Wigner mappings (2.16) and using the CCR we obtain exemplarily,

$$\begin{aligned}
\left[\alpha\hat{a}_i + \beta\hat{a}_l, \hat{a}_k\right]_{q^-} =& \left(\alpha\hat{a}_i + \beta\hat{a}_l\right)\hat{a}_k - \exp(i\theta)\hat{a}_k\left(\alpha\hat{a}_i + \beta\hat{a}_l\right) \\
=& \alpha\left[\hat{a}_i, \hat{a}_k\right]_{q^-_{i,k}} + \beta\left[\hat{a}_l, \hat{a}_k\right]_{q^-_{l,k}}, \quad \text{if} \quad i < l < k. \\
\left[\alpha\hat{a}_i + \beta\hat{a}_l, \hat{a}_k\right]_{q^-} =& \left(\alpha\hat{a}_i + \beta\hat{a}_l\right)\hat{a}_k - \exp(-i\theta)\hat{a}_k\left(\alpha\hat{a}_i + \beta\hat{a}_l\right) \\
=& \alpha\left[\hat{a}_i, \hat{a}_k\right]_{q^-_{i,k}} + \beta\left[\hat{a}_l, \hat{a}_k\right]_{q^-_{l,k}}, \quad \text{if} \quad k < l < i.
\end{aligned} \tag{2.31}$$

While on the other hand

$$\begin{aligned}
\left[\alpha\hat{a}_i + \beta\hat{a}_l, \hat{a}_k\right]_{q^-} =& \left(\alpha\hat{a}_i + \beta\hat{a}_l\right)\hat{a}_k - q^-\hat{a}_k\left(\alpha\hat{a}_i + \beta\hat{a}_l\right) \\
\neq& \alpha\left[\hat{a}_i, \hat{a}_k\right]_{q^-_{i,k}} + \beta\left[\hat{a}_l, \hat{a}_k\right]_{q^-_{l,k}}, \quad \text{if} \quad l < k < i.
\end{aligned} \tag{2.32}$$

This circumstance also results in the specific anti-symmetrization of the deformed commutators, which depends again on the way the ordered set is defined on the lattice.

$$\left[A_i, B_j\right]_{q^{\pm}_{i,j}} = -q^{\pm}_{i,j}\left[B_j, A_i\right]_{q^{\mp}_{j,i}} \tag{2.33}$$

This is in contrast to the usual anti-symmetry which is valid for an ordinary Lie-algebra,

$$\left[A_i, B_j\right] = -\left[B_j, A_i\right]. \tag{2.34}$$

A very important point is also that, in one-dimensional systems, the Jordan-Wigner string does not induce a change in the range of interactions present in the system, even though it is a non-local operator [19]. This means that a transmutation of the exchange statistics results only in a change of the form of the interaction while its short-range character stays conserved. This means, that in a broader sense, the particle statistics becomes insignificant in one dimension.

### 2.2.3 Bosonic Representation

Before the Jordan-Wigner transformation is applied to the Anyon-Hubbard model, one should choose a set of boundary conditions, i.e. periodic or open, as it results in unitarily non-equivalent Hamiltonians. As this circumstance is profusely neglected in the literature, we nevertheless list both transformations for open, as well as periodic boundary conditions

$$\hat{H}_-^{\mathrm{OBC}} = \frac{U}{2}\sum_{i=1}^{L}\hat{n}_i\left(\hat{n}_i - 1\right) - J\sum_{i=1}^{L-1}\left[\hat{b}_i^\dagger\hat{b}_{i+1}\exp(i\theta\hat{n}_i) + \mathrm{h.c.}\right] - \mu\sum_{i=1}^{L}\hat{n}_i \tag{2.35}$$

$$\hat{H}_{+}^{\mathrm{OBC}} = \frac{U}{2}\sum_{i=1}^{L}\hat{n}_i\left(\hat{n}_i-1\right) - J\sum_{i=1}^{L-1}\left[\hat{b}_{i+1}^{\dagger}\hat{b}_i\exp(i\theta\hat{n}_{i+1}) + \mathrm{h.c.}\right] - \mu\sum_{i=1}^{L}\hat{n}_i \tag{2.36}$$

$$\begin{aligned}\hat{H}_{-}^{\mathrm{PBC}} =& \frac{U}{2}\sum_{i=1}^{L}\hat{n}_i\left(\hat{n}_i-1\right) - J\sum_{i=1}^{L-1}\left[\hat{b}_{i}^{\dagger}\hat{b}_{i+1}\exp(i\theta\hat{n}_{i}) + \mathrm{h.c.}\right] - \mu\sum_{i=1}^{L}\hat{n}_i \\ & - J\left[\exp(i\theta(\hat{N}-1))\hat{b}_L^{\dagger}\hat{b}_1\exp(i\theta\hat{n}_L) + \mathrm{h.c.}\right]\end{aligned} \tag{2.37}$$

$$\begin{aligned}\hat{H}_{+}^{\mathrm{PBC}} =& \frac{U}{2}\sum_{i=1}^{L}\hat{n}_i\left(\hat{n}_i-1\right) - J\sum_{i=1}^{L-1}\left[\hat{b}_{i+1}^{\dagger}\hat{b}_{i}\exp(i\theta\hat{n}_{i+1}) + \mathrm{h.c.}\right] - \mu\sum_{i=1}^{L}\hat{n}_i \\ & - J\left[\exp(-i\theta(\hat{N}-1))\hat{b}_1^{\dagger}\hat{b}_L\exp(i\theta\hat{n}_1) + \mathrm{h.c.}\right]\end{aligned} \tag{2.38}$$

These Hamiltonians are almost identical to the Bose-Hubbard Hamiltonian, to which they reduce to in the limit $\theta \to 0$, except the conditional hopping amplitudes they posses. Depending on the choice of tail orientation for the disorder operator [30][31], the hopping process from one site to the next depends either on the occupation of the former respectively the following site. It should be noted that even the Hamiltonian operators are complex, they are nevertheless hermitian, which implies real eigenvalues. Remarkably, even in the limit of vanishing on-site interactions $U \to 0$ the resulting Hamiltonians remains off-diagonal in both position- or momentum-representation, which corresponds to the presence of an intrinsic many-body interaction[5], a characteristic feature of anyons.

## 2.3 Experimental realization

In the following part three different experimental proposals for the implementation of the Anyon-Hubbard model in a one-dimensional optical lattice are briefly reviewed. The common feature of these proposals is the achievement of the density-dependent Peierls phase in the correlated hopping, which can be viewed as the bosonic pendant to the anyonic braiding in one dimension. But they differ, for example, in their parameter range or dimension of the local Hilbert space.

### 2.3.1 Assisted Raman-Tunneling 1

The first proposal in Ref. [1] is based on an assisted Raman-tunneling scheme. The optical lattice is tilted with an energy off-set $\Delta$ between adjacent sites, inducing the parity violation which is inherent to anyonic systems. For low densities, the local occupation can be restricted to up to two particles per site. As an empty lattice site does not contribute to the density-dependent Peierls phase, there is an effective four-dimensional ground-state manifold for two neighboring sites. It is now assumed that the two states on one site are coupled via an excited state $|\, e \,\rangle$ and four external driving fields labeled 1,2,3,4 in Fig. 2.1 with the two corresponding states on the other site. According to this notation the fields 1 and 2 couple $|\, e \,\rangle$ to the left-hand side, while fields

3 and 4 couple $|\,e\,\rangle$ to the right-hand side. This configuration could be experimentally realized for $^{87}$Rb with two lattices. The first lattice corresponds to the ground state and would trap atoms in the $F = 1$, $m_F = -1$ hyperfine state, while the second lattice acts on $F = 1$, $m_F = 0$ states and allows to realize $|\,e\,\rangle$ as a vibrational state. Particles in the state $|\,e\,\rangle$ would then be trapped between two wells of the first underlying optical lattice, but not necessarily in their middle. The advantage of this approach lies in its resolvability, because the energy scale of the external fields is in the radio-frequency regime, which is the same order of magnitude as the system energy scales. Similar to the proposal by Ref. [32], the tilting energy $\Delta$ can effectively be gauged away within an adiabatic elimination of the excited state $|\,e\,\rangle$, yielding an effective Hamiltonian without the tilting which couples both neighboring sites. In order to match the conditional hopping expression of the Anyon-Hubbard model, the following conditions have to be imposed on the effective tunneling rates with effective complex valued Rabi-frequencies,

$$\begin{aligned} J_{23} &= J_{24} \equiv J, \\ J_{13} &= J_{14} \equiv J\exp(i\theta), \end{aligned} \tag{2.39}$$

where $\theta$ corresponds again to the statistical parameter of the anyonic system. These conditions can be met by taking advantage of the tunabillity of each driving field, see Ref. [1].

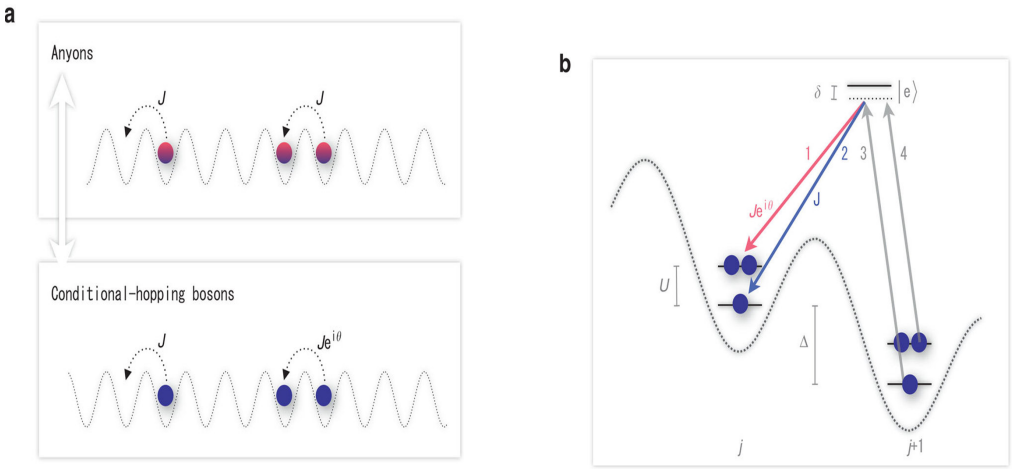


**(a)** Schemata of the equivalence of bosonic conditional hopping and anyonic braiding in 1*d*.

**(b)** Assisted Raman coupling of the two wells, inducing the density dependent phase-shift.

**FIG. 2.1:** Implementation of density-dependent Peierls phase via Raman coupling according to the proposal of Ref. [1]

It should be noted that this experimental proposal is subject to specific restrictions, which are certainly not fulfilled by the Anyon-Hubbard model. For example the maximal occupancy

is restricted to two particles per site. Additionally the parameter regime, where the Raman coupling is achievable, is restricted to a certain interval of the energy scale of the system, as explained in detail in Ref. [1].

### 2.3.2 Assisted Raman-Tunneling 2

The next proposal [22] aims to improve the first scenario and additionally gives rise to controllable effective interactions in the system. The basic idea of this implementation is to use bosons or fermions occupying two possible states, say $|A\rangle$ and $|B\rangle$, in a deeply tilted spin-independent lattice, where hopping processes are suppressed. Now both states can be coupled far off-resonance by lasers with linear polarization $L_1$, $L_4$ as well as circular polarization $L_2$, $L_3$. These lasers can induce the Raman-assisted hopping processes between the different states as depicted in FIG. 2.2.

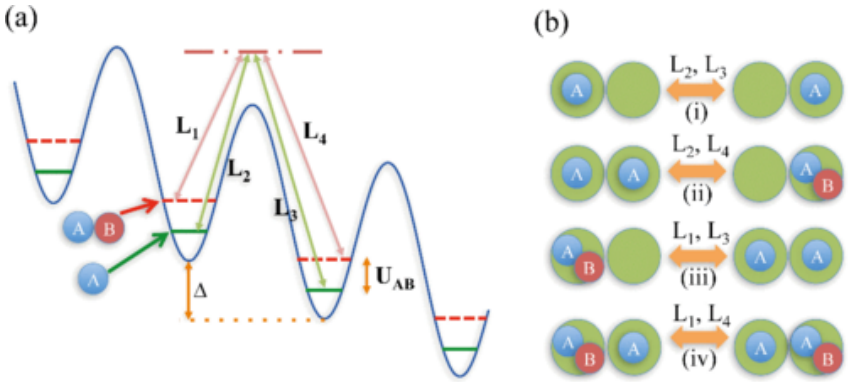


**(a)** Raman scheme proposed to implement the Anyon Hubbard model.

**(b)** Raman-assisted hopping processes, coupling the states $|A\rangle$, $|B\rangle$ at two adjacent sites.

**FIG. 2.2:** Graphical representation of the involved Raman processes in Ref. [22]

In FIG. 2.2 (a) $L_i$ denotes the four different lasers, coupling nearest sites, as well as the two different states which interact with the strength $U_{AB}$, in a lattice with a tilt that is denoted by $\Delta$. In FIG. 2.2 (b) the different Raman-assisted hops are depicted with the laser frequencies chosen such that

$$\begin{aligned} (i) &: \omega_2 - \omega_3 = -\Delta \\ (ii) &: \omega_2 - \omega_4 = -\Delta + U_{AB} + U \\ (iii) &: \omega_1 - \omega_3 = -\Delta - U_{AB} - U \\ (iv) &: \omega_1 - \omega_4 = -\Delta \end{aligned} \tag{2.40}$$

The frequency differences do now compensate the lattice tilt in order to avoid Bloch oscillations, and deliver an effective, controllable on-site interaction via the detuning $U$. If now the width $W$ of the Raman resonances is narrow enough, then each process can be adressed independently.

Additionally, in order to avoid the following undesirable processes for bosons

$$\begin{aligned}(1) &: (A,0) \longrightarrow (0,B)\\ (2) &: (A,A) \longrightarrow (0,AA)\\ (3) &: (AB,A) \longrightarrow (B,AA)\end{aligned} \tag{2.41}$$

the parameters have to be chosen such that $U_{AA}-U_{AB}, U_{AA}, U_{AB} \gg W$. Finally, if now the Rabi frequencies characterizing the lasers $L_i$ are chosen such that they mimic bosonic enhancement, this system can be mapped to a Bose-Hubbard model with a density-dependent Peierls phase, which again can be identified with the Anyon-Hubbard model. Note that both proposals [1, 22] have in common to implement the conditional hopping with Raman-assisted tunneling processes. But, whereas proposal [1] realizes the restriction of having up to two particles per site via a Feshbach resonance, the scheme [22] allows naturally controllable effective interactions.

### 2.3.3 Floquet Realization

The most recent proposal of Ref. [23] aims to simplify the experimental set up by not relying on Raman assisted tunneling processes. Instead the conditional hopping process is realized by a combination of lattice tilting and a periodic driving. This is described by the following Hamiltonian

$$\hat{H}(t) = \sum_{j=1}^{L} -J'\Big(\hat{b}_j^\dagger \hat{b}_{j-1} + \text{h.c.}\Big) + \frac{U'\hat{n}_j(\hat{n}_j-1)}{2} + V_j\hat{n}_j + [\Delta + F(t)]\, j\hat{n}_j, \tag{2.42}$$

where $J'$ and $U'$ are the tunneling rate and the interaction strength, respectively, whereas $\Delta$ characterizes the potential tilt. Additionally $V_j$ denotes a weak additional on-site potential whereas $F(t) = F(t+T)$ represents an external periodic potential. Now the parameters are chosen such that the following requirements are fulfilled see Fig. 2.3,

$$\Delta = \hbar\omega \quad , \quad U' = 2\hbar\omega + U, \tag{2.43}$$

$$J', U', \mid V_j - V_{j-1} \mid \ll \hbar\omega. \tag{2.44}$$

Here (2.43) is a resonance condition, while (2.44) can be viewed as a high frequency condition.

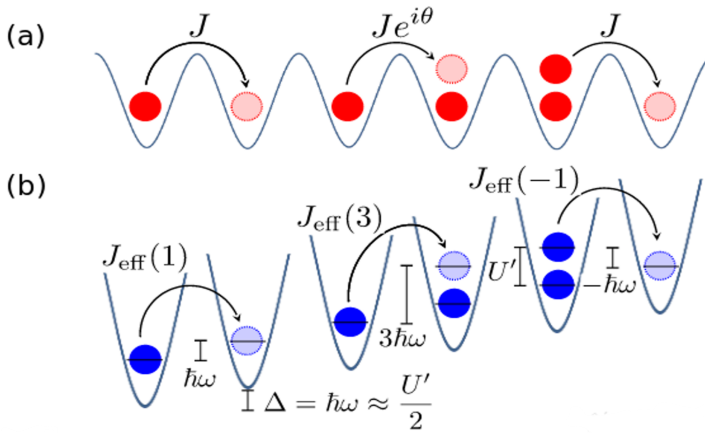


**(a)** Number-dependent tunneling process involving a maximal occupancy of two particles per site.

**(b)** Equivalent "photon"-processes in the tilted lattice with strong on-site interaction.

**FIG. 2.3:** Realization of the conditional hopping process by tilting and driving the optical lattice in Ref. [23]

If these conditions are fulfilled, the dominant part of the local interaction is given by $\hat{H}_0 = \hbar\omega \sum_{j=1}^{L} [\hat{n}_j(\hat{n}_j - 1) + j\hat{n}_j]$, so that tunneling processes are energetically disfavored, which is manifested in the energy cost of hopping from well $j$ to $j-1$, $\hbar\omega\nu_{j,j-1} = \pm\hbar\omega, \pm 3\hbar\omega, \ldots$ with $\nu_{j,j-1} = 2\,(\hat{n}_j - \hat{n}_{j-1}) + 3$ . The main idea is now to induce these coherent hopping processes by the driving force, which periodically absorbs respectively provides the energy quanta of absolute value $\hbar\omega$, where the dependence on the onsite-density is given by the matrix elements $\nu_{j,j-1}$. Now by applying Floquet theory in the high frequency approximation to leading order, as well as a time-dependent gauge transformation, one obtains the following effective Hamiltonian,

$$\hat{H}_{\text{eff}} = \sum_{j=1}^{L} \left[\hat{b}_j^\dagger J_{\text{eff}}(\nu_{j,j-1})\hat{b}_{j-1} + \text{h.c.}\right] + \frac{U\hat{n}_j(\hat{n}_j - 1)}{2} + V_j\hat{n}_j. \tag{2.45}$$

Here the effective hopping matrix element stems from

$$\begin{aligned} J_{\text{eff}}(\nu) &= J/T \int_0^T dt \exp(i\omega\nu t - i\chi(t)) \\ \chi(t) &= -\frac{1}{\hbar}\int_0^\tau d\tau F(\tau). \end{aligned} \tag{2.46}$$

There is now still the freedom to choose $\chi(t)$ in such a way that the hopping processes mimics the ones of the Anyon-Hubbard model, by assuming $\chi(t) = A\cos(\omega t) + B\cos(2\omega t)$ with appropriate amplitudes A,B it is possible to adjust a suitable statistical parameter $\theta$. The tunable interaction parameter $U$ as well as $J_{\text{eff}}$ can take both positive and negative values, which is not the case for the Anyon-Hubbard model.

As a concluding remark, it should be noted that these three proposals, do not provide an explicit realization of the Anyon-Hubbard model, they just provide a realization of certain sub-cases. Consider for example the proposal of [23], here the maximal occupancy per site is not restricted a priori, but as the system parameters can be chosen to be negative, i.e. $U < 0$ ,the resulting system would be unstable, at least for some parameter ranges. In opposition the proposal of [1], does not allow negative parameters, which would be consistent with the tight-binding approximation, but restricts the number of particles per site.

# 3 Symmetries

In the following chapter we examine the classical symmetries of the bosonic Hamiltonians (2.30)–(2.33). Before we start, we would like to mention, that all these Hamiltonians conserve the total number of particles, which means $\left[\hat{H}, \hat{N}\right] = 0$. The dynamical symmetry group of these Hamiltonians is spanned by the normally ordered operators $\hat{b}_i^\dagger \hat{b}_j$ with $i,j \in \{1,...,\mathrm{L}\}$, and is equivalent to $SU(L)$ [33], which is the special unitary group of degree $L$. As this symmetry is not inherently connected to the concept of anyons, our focus will be on space-time symmetries in the following.
If one considers the limit of $\theta \longrightarrow 0$, the Hamiltonians reduce to Bose-Hubbard Hamiltonians with open or periodic boundary conditions, respectively. Then, in the case of open boundary conditions, the only spatial symmetry is the invariance under a parity transformation, while for periodic boundary conditions the system is additionally translational invariant. In the following the impact of the conditional hopping on these symmetries is studied in detail.

## 3.1 Spatial Symmetries

In order to derive the response of (2.31) or (2.32) to spatial transformations in detail, its necessary to obtain the corresponding generators in explicit form. Since the model is defined on a lattice, every spatial transformation can be generated by a sequence of permutations of the site indices. The set of all such permutations of $L$ elements forms the symmetric group $S_L$. Thus if one would have a representation of this group in terms of bosonic operators, the operators representing the spatial transformations could be constructed explicitly [24].

### 3.1.1 Transposition Operators

Since the symmetric group $S_L$ can be generated by elementary transpositions, its sufficient to define these in terms of bosonic operators. The corresponding transposition operators can be written as,[25]

$$\hat{T}_{i,j} = -i\exp\left(i\frac{\pi}{2}\hat{R}_{i,j}\right)\exp\left(i\frac{\pi}{2}\hat{S}_{i,j}\right), \tag{3.1}$$

$$\hat{R}_{i,j} = \hat{b}_i^\dagger \hat{b}_j + \mathrm{h.c.} \tag{3.2}$$

$$\hat{S}_{i,j} = 1 - \hat{n}_i - \hat{n}_j. \tag{3.3}$$

With the following properties

$$\hat{T}_{i,j}^{\dagger} = \hat{T}_{i,j}^{-1}, \tag{3.4}$$
$$\hat{T}_{i,i} = 1, \tag{3.5}$$
$$\hat{T}_{i,j} = \hat{T}_{j,i}. \tag{3.6}$$

A short calculation reveals the action of the transposition operators on bosonic lattice operators,

$$\hat{T}_{i,j}\hat{b}_j\hat{T}_{i,j}^{\dagger} = \hat{b}_i, \quad \hat{T}_{i,j}\hat{b}_j^{\dagger}\hat{T}_{i,j}^{\dagger} = \hat{b}_i^{\dagger}, \tag{3.7}$$
$$\hat{T}_{i,j}\hat{b}_i\hat{T}_{i,j}^{\dagger} = \hat{b}_j, \quad \hat{T}_{i,j}\hat{b}_i^{\dagger}\hat{T}_{i,j}^{\dagger} = \hat{b}_j^{\dagger}, \tag{3.8}$$

which represents indeed a transposition of the site indices. One can show that the operators satisfy the following relations

$$\hat{T}_{i,j}\hat{T}_{j,k} = \hat{T}_{i,k}\hat{T}_{i,j} = \hat{T}_{j,k}\hat{T}_{i,k} \;\; ; \; i \neq j \neq k \neq i, \tag{3.9}$$
$$\hat{T}_{i,j}^2 = 1, \tag{3.10}$$
$$\left[\hat{T}_{i,j}, \hat{T}_{k,l}\right] = 0 \;\; ; \; i,j \neq k,l. \tag{3.11}$$

Eqs.(3.9)–(3.11) can be used to define the generators of $S_L$, with which one can construct any spatial transformation on the lattice.

### 3.1.2 Shift operator

If one considers periodic boundary conditions for the Anyon-Hubbard model (2.1), the system looks homogeneous which would imply translational invariance. Nevertheless a closer look at the bosonic Hamiltonians (2.31) and (2.32) is needed in order to reveal their behavior under a shift of the lattice sites. The so called shift operator induces these spatial shifts and is mathematically a representation of the generator of the cyclic subgroup of order $L$ of the symmetric group $S_L$

$$\hat{U}_n = \hat{T}_{n-1,n} \ldots \hat{T}_{2,3}\hat{T}_{1,2}\,, \quad \text{for} \quad n = 2, \ldots, L. \tag{3.12}$$

The action of $\hat{U}_L$ on the bosonic operators is defined in the following

$$\begin{aligned} \hat{U}_L\hat{b}_j &= \hat{b}_{j-1}\hat{U}_L, \quad j = 2, \ldots L, \\ \hat{U}_L\hat{b}_j &= \hat{b}_L\hat{U}_{L,}\,, \quad\;\; j = 1, \end{aligned} \tag{3.13}$$

which clearly represents a shift of the spatial index from $j$ to $j-1$ for $j \in [1, L]$. Consequently $\hat{U}_L^\dagger$ induces a shift from $j$ to $j+1$. Out of this property it is already clear that

$$\begin{aligned} \hat{U}_L^\dagger \hat{U}_L &= 1, \\ \hat{U}_L^L &= 1. \end{aligned} \tag{3.14}$$

With the help of these relations we can calculate the action of $\hat{U}_L$ on $\hat{H}_-^{\mathrm{PBC}}$ and $\hat{H}_+^{\mathrm{PBC}}$ explicitly In the following we focus on the hopping term, as the onsite terms are trivially invariant under a spatial shift and thus can be neglected

$$\begin{aligned} \hat{U}_L^\dagger \hat{H}_{+,\mathrm{hop}}^{\mathrm{PBC}} \hat{U}_L = &- J \sum_{i=1}^{L-2} \left[ \hat{b}_{i+1}^\dagger \hat{b}_i \exp(i\theta \hat{n}_{i+1}) + \mathrm{h.c.} \right] - J \left[ \hat{b}_1^\dagger \hat{b}_L \exp(i\theta \hat{n}_1) + \mathrm{h.c.} \right] \\ &- J \left[ \exp(-i\theta(\hat{N}-1)) \hat{b}_L^\dagger \hat{b}_{L-1} \exp(i\theta \hat{n}_1) + \mathrm{h.c.} \right] \end{aligned} \tag{3.15}$$

$$\begin{aligned} \hat{U}_L^\dagger \hat{H}_{-,\mathrm{hop}}^{\mathrm{PBC}} \hat{U}_L = &- J \sum_{i=1}^{L-2} \left[ \hat{b}_i^\dagger \hat{b}_{i+1} \exp(i\theta \hat{n}_i) + \mathrm{h.c.} \right] - J \left[ \hat{b}_L^\dagger \hat{b}_1 \exp(i\theta \hat{n}_L) + \mathrm{h.c.} \right] \\ &- J \left[ \exp(i\theta(\hat{N}-1)) \hat{b}_{L-1}^\dagger \hat{b}_L \exp(i\theta \hat{n}_1) + \mathrm{h.c.} \right] \end{aligned} \tag{3.16}$$

The equations (3.15) and (3.16) show that the hopping operators are in general not invariant under spatial shifts, as the special phase term at the boundary is shifted to the former site. Nevertheless, as $\theta$ can be any fraction of $\pi$, there can be translationally invariant phases for special values of $\theta$ and $\hat{N}$, which obviously reduces to the case $\theta \longrightarrow 0$ if the thermodynamic limit is approached.
Another example is provided by the case $\theta = \pi$. It should be treated in detail, as it reveals the pseudo-fermionic character of the bosonic Hamiltonians with correlated hopping. To this end we focus solely on the boundary terms,

$$\hat{H}_{-,\mathrm{hop}}^{\mathrm{PBC}} - J \sum_{i=1}^{L-1} \left[ (-1)^{\hat{n}_i} \hat{b}_i^\dagger \hat{b}_{i+1} + \mathrm{h.c.} \right] = - J (-1)^{\hat{N}-1} \left[ (-1)^{\hat{n}_L} \hat{b}_L^\dagger \hat{b}_1 + \mathrm{h.c.} \right], \tag{3.17}$$

$$\hat{H}_{+,\mathrm{hop}}^{\mathrm{PBC}} - J \sum_{i=1}^{L-1} \left[ (-1)^{\hat{n}_{i+1}} \hat{b}_{i+1}^\dagger \hat{b}_i + \mathrm{h.c.} \right] = - J (-1)^{\hat{N}-1} \left[ (-1)^{\hat{n}_1} \hat{b}_1^\dagger \hat{b}_L + \mathrm{h.c.} \right]. \tag{3.18}$$

Equations (3.17) and (3.18) show that in the case $\theta = \pi$, there are two possibilities, which depend on the total number of particles $\hat{N}$. If the total number of particles is even, the sign in front of the boundary term switches from minus to plus, which corresponds to anti-periodic boundary conditions. Whereas if the total number of particles is odd, the sign remains unaffected, and translational invariance is recovered.

### 3.1.3 Parity

Anyonic systems have to break parity irrespective of any boundary conditions, which can be already seen at the level of the deformed commutation relations (2.2). Our goal is now to prove

that explicitly on the level of the bosonic Hamiltonians, and with that uncover the relation between the two kinds of tail-orientation of the Jordan-Wigner transformation. We can define again the operator mediating the parity transformation via a sequence of elementary transpositions [24],

$$\hat{R}_L = \hat{U}_2 \dots \hat{U}_L, \tag{3.19}$$

where $\hat{U}_L$ is again the shift operator defined in the previous subsection. The parity operator induces an index shift of the bosonic operators from site $j$ to site $L-j+1$, which has the following consequences on let us say $\hat{H}^{\mathrm{OBC}}_{-,\mathrm{hop}}$. Again we neglect any on-site terms as they transform trivially under this transformation

$$\begin{aligned}
\hat{R}_L^\dagger \hat{H}^{\mathrm{OBC}}_{-,\mathrm{hop}} \hat{R}_L =& -J\sum_{i=1}^{L-1}\left[\hat{b}^\dagger_{L-i+1}\hat{b}_{L-i}\exp(i\theta\hat{n}_{L-i+1}) + \mathrm{h.c.}\right] \\
=& -J\sum_{i=-L}^{-2}\left[\hat{b}^\dagger_{-i}\hat{b}_{-(i+1)}\exp(i\theta\hat{n}_{-i}) + \mathrm{h.c.}\right] \\
=& -J\sum_{i=2}^{L}\left[\hat{b}^\dagger_{i}\hat{b}_{(i-1)}\exp(i\theta\hat{n}_{i}) + \mathrm{h.c.}\right] \\
=& -J\sum_{i=1}^{L-1}\left[\hat{b}^\dagger_{i+1}\hat{b}_{i}\exp(i\theta\hat{n}_{i+1}) + \mathrm{h.c.}\right] = \hat{H}^{\mathrm{OBC}}_{+,\mathrm{hop}}
\end{aligned} \tag{3.20}$$

This proves that the Jordan-Wigner strings are parity transforms of each other, where $\hat{R}_L^\dagger = \hat{R}_L^{-1}$ and thus $\hat{H}^{\mathrm{OBC}}_{-,\mathrm{hop}}$ and $\hat{H}^{\mathrm{OBC}}_{+,\mathrm{hop}}$ are unitarily equivalent. The same is obviously true for periodic boundary condition, where the same relation holds for the two different choices of tail-orientation. As a final remark, it should be noted that in the limit $\theta \longrightarrow 0, \pi$, the deformed commutation relations (2.17)–(2.19) become again invariant under parity transformation as well as the Hamiltonians (2.30)–(2.33). Furthermore for special values of $\theta$ and $\hat{n}_i$ it can happen that $\hat{R}_L^\dagger \hat{H}^{\mathrm{OBC}}_{-,\mathrm{hop}} \hat{R}_L = -\hat{H}^{\mathrm{OBC}}_{-,\mathrm{hop}}$, which means that the hopping terms have a well defined odd parity under spatial inversion and thus $\hat{R}_L$ is a chiral symmetry operation, i.e. $\left\{\hat{H}_{\mathrm{hop}}, \hat{R}_L\right\} = 0$.

## 3.2 Time Reversal

In this section, the connection between anyonic exchange statistics and time reversal symmetry will be discussed. With a time reversal transformation, we mean a reflection of the time coordinate $t \longrightarrow -t$. In classical mechanics such a transformation reverses the sign of momentum variables $p \longrightarrow -p$, while keeping the position variables unchanged $x \longrightarrow x$. If we want to

translate this to the quantum mechanical setting, we should demand a conservation of the $CCR$ under this transformation. This can only be fulfilled if the time reversal operator $\hat{T}$ is antiunitary, and thus antilinear, which implies $\hat{T}i\hat{T}^{-1} = -i$. It turns out, that for spinless particles, this operator corresponds to the complex conjugation operator $\hat{T} = \hat{K}$ [34]. Thus the action of this operator on the second quantized bosonic creation and annihilation operators in position and momentum space is

$$\begin{aligned} &\hat{T}\hat{b}_i\hat{T}^{-1} = \hat{b}_i, \\ &\hat{T}\hat{b}_k\hat{T}^{-1} = \hat{T}\left[\frac{1}{\sqrt{L}}\sum_{i=1}^{L}\hat{b}_i\exp(ikl)\right]\hat{T}^{-1} = \hat{b}_{-k}, \end{aligned} \tag{3.21}$$

which is in agreement with the classical case. Now by looking at the deformed commutation relations (2.2), it is again clear that they intrinsically break the time-reversal symmetry by a complex conjugation of the phase term, except for the special cases $\theta \longrightarrow 0, \pi$. The same holds also for the bosonic Hamiltonians (2.30)-(2.33), leading to

$$\hat{T}\hat{H}_{-}^{\mathrm{OBC}}\hat{T}^{-1} = \frac{U}{2}\sum_{i=1}^{L}\hat{n}_i\left(\hat{n}_i - 1\right) - J\sum_{i=1}^{L-1}\left[\hat{b}_i^{\dagger}\hat{b}_{i+1}\exp(-i\theta\hat{n}_i) + \mathrm{h.c.}\right] - \mu\sum_{i=1}^{L}\hat{n}_i \tag{3.22}$$

$$\hat{T}\hat{H}_{+}^{\mathrm{OBC}}\hat{T}^{-1} = \frac{U}{2}\sum_{i=1}^{L}\hat{n}_i\left(\hat{n}_i - 1\right) - J\sum_{i=1}^{L-1}\left[\hat{b}_{i+1}^{\dagger}\hat{b}_i\exp(-i\theta\hat{n}_{i+1}) + \mathrm{h.c.}\right] - \mu\sum_{i=1}^{L}\hat{n}_i \tag{3.23}$$

$$\begin{aligned} \hat{T}\hat{H}_{-}^{\mathrm{PBC}}\hat{T}^{-1} =& \frac{U}{2}\sum_{i=1}^{L}\hat{n}_i\left(\hat{n}_i - 1\right) - J\sum_{i=1}^{L-1}\left[\hat{b}_i^{\dagger}\hat{b}_{i+1}\exp(-i\theta\hat{n}_i) + \mathrm{h.c.}\right] - \mu\sum_{i=1}^{L}\hat{n}_i \\ &- J\left[\exp(-i\theta(\hat{N}-1))\hat{b}_L^{\dagger}\hat{b}_1\exp(-i\theta\hat{n}_L) + \mathrm{h.c.}\right] \end{aligned} \tag{3.24}$$

$$\begin{aligned} \hat{T}\hat{H}_{+}^{\mathrm{PBC}}\hat{T}^{-1} =& \frac{U}{2}\sum_{i=1}^{L}\hat{n}_i\left(\hat{n}_i - 1\right) - J\sum_{i=1}^{L-1}\left[\hat{b}_{i+1}^{\dagger}\hat{b}_i\exp(-i\theta\hat{n}_{i+1}) + \mathrm{h.c.}\right] - \mu\sum_{i=1}^{L}\hat{n}_i \\ &- J\left[\exp(i\theta(\hat{N}-1))\hat{b}_1^{\dagger}\hat{b}_L\exp(-i\theta\hat{n}_1) + \mathrm{h.c.}\right] \end{aligned} \tag{3.25}$$

Out of (3.22)–(3.25), as well as the results of section 3.1.3, it is already clear that also the combined symmetry operation of parity and time-reversal $\hat{R}_L\hat{T}$ is not a symmetry of the Hamiltonians (2.30)–(2.33) in general. Nevertheless for some values of the onsite density $\hat{n}_i$ and $\theta$ the invariance under the combined symmetry operation of $\hat{R}_L\hat{T}$ could in principle be restored. This can be observed at the level of commutation relations, i.e.

$$\begin{aligned} &\left(\hat{R}_L\hat{T}\right)^{\dagger}\left\{\hat{a}_i\hat{a}_j - \exp\left[i\theta\mathrm{sgn(i-j)}\right]\hat{a}_j\hat{a}_i\right\}\left(\hat{R}_L\hat{T}\right) \\ &= \left\{\hat{a}_{L-i+1}\hat{a}_{L-j+1} - \exp\left[-i\theta\mathrm{sgn(i-j)}\right]\hat{a}_{L-j+1}\hat{a}_{L-i+1}\right\}. \end{aligned} \tag{3.26}$$

In Eq. (3.26) it can be seen that the deformed commutation relation are invariant under combined time-reversal and parity transformation, in the sense that the time reversal induces a complex conjugation but the parity transform reverses the spatial order on the one-dimensional line and thus the phase the particles acquire when they exchange remains the same. As an example we choose a constant density $\hat{n}_i|\,\Psi\,\rangle = 1|\,\Psi\,\rangle = \hat{n}_{i+1}|\,\Psi\,\rangle$ and $\theta = \frac{\pi}{2}$ for $\hat{H}_{-}^{\mathrm{OBC}}$, where it is again sufficient to restrict the discussion to the hopping term.

$$\begin{aligned}\hat{H}_{-,\mathrm{hop}}^{\mathrm{OBC}}\left(\frac{\pi}{2},1\right) &= -iJ\sum_{i=1}^{L-1}\left[\hat{b}_i^{\dagger}\hat{b}_{i+1} - \mathrm{h.c.}\right] = \hat{T}^{\dagger}\hat{H}_{+,\mathrm{hop}}^{\mathrm{OBC}}\left(\frac{\pi}{2},1\right)\hat{T} \\ &= \left(\hat{R}_L\hat{T}\right)^{\dagger}\hat{H}_{-,\mathrm{hop}}^{\mathrm{OBC}}\left(\frac{\pi}{2},1\right)\left(\hat{R}_L\hat{T}\right)\end{aligned} \tag{3.27}$$

The crucial point is that for $\theta = 0, \pi$ the hopping part of the Hamiltonians have a well defined parity with respect to time-reversal namely an even one, whereas this is not the case for $0 < \theta < \pi$ and arbitrary $\hat{n}_i$ in general. Nevertheless an odd parity under time-reversal, i.e. a chiral symmetry $\left\{\hat{H}_{\mathrm{hop}}, \hat{T}\right\} = 0$, can be realized at least for some parameter values as can be seen in Eq. (3.27). Thus we conclude that if the hopping terms posses an odd parity with respect to spatial inversion, as well as time-reversal, then the Hamiltonians are invariant under the combined symmetry operation $\left[\hat{H}, \hat{R}_L\hat{T}\right] = 0$.

## 3.3 Bosonic Shiba Transformation

In the last section of chapter 3, we quickly discuss the bosonic version of the Shiba transform $\hat{S}$ [24], which basically represents a local gauge transformation, with the following action on the bosonic operators

$$\hat{S}^{\dagger}\hat{b}_i\hat{S} = (-1)^i\,\hat{b}_i, \tag{3.28}$$

Thus, this transformation reverses the sign in front of hopping terms $J \longrightarrow -J$ of the Hamiltonians with correlated hopping, if the following boundary conditions are fulfilled: $(i)$ open boundary conditions, or $(ii)$ periodic boundary conditions with an even number of sites. Of course this unitary transformation is not a symmetry of the Hamiltonians (2.30)–(2.33) for a non-zero $J$ in general, but can connect some cases with specific values of the statistical parameter $\theta$, as well as deriving predictions on the perturbative treatment of them [35].
Let us consider as an example the special case where the onsite-density $\hat{n}_i$ is fixed to a certain value $\hat{n}_i = n_0$, thus the kinetic term for open boundary and $\theta = \pi$ is given by

$$\hat{H}_{-,\mathrm{hop}}^{OBC}(\theta = \pi, n_0) = -J\sum_{i=1}^{L-1}\left((-1)^{n_0}\hat{b}_i^{\dagger}\hat{b}_{i+1} + \mathrm{h.c.}\right) = \hat{H}_{+,\mathrm{hop}}^{OBC}(\theta = \pi, n_0) \tag{3.29}$$

Thus it can be seen that, if $n_0$ is even, the pseudo-fermionic case is equivalent to its bosonic pendant $\theta = 0$

$$\hat{H}_{\mathrm{hop}}^{\mathrm{OBC}}(\theta = \pi, n_0 = \mathrm{even}) \equiv \hat{H}_{\mathrm{hop}}^{\mathrm{OBC}}(\theta = 0, n_0 = \mathrm{even}) \tag{3.30}$$

whereas if $n_0$ is odd they differ in the sign in front of the hopping term. Nevertheless, as open boundary conditions are assumed, the Shiba transform still relates the latter case and its bosonic pendant, thus they are still unitarily equivalent and with that isospectral

$$\hat{S}^\dagger \hat{H}_{hop}^{OBC}(\theta = \pi, n_0 = \text{odd})\hat{S} = \hat{H}_{hop}^{OBC}(\theta = 0, n_0 = \text{odd}). \tag{3.31}$$

Furthermore the combined operations of $\hat{S}\hat{T}$ as well as $\hat{S}\hat{R}_L$ can be symmetries for some parameter values, if the requirements on the boundaries are fulfilled and the hopping terms are odd with respect to both discrete symmetry operations. As an example we choose again $\hat{n}_i|\,\Psi\,\rangle = 1|\,\Psi\,\rangle = \hat{n}_{i+1}|\,\Psi\,\rangle$ and $\theta = \frac{\pi}{2}$ for $\hat{H}_-^{\text{OBC}}$ and concentrate only on the kinetic energy term,

$$\begin{aligned}\hat{H}_{-,\text{hop}}^{\text{OBC}}\left(\frac{\pi}{2},1\right) &= -iJ\sum_{i=1}^{L-1}\left[\hat{b}_i^\dagger \hat{b}_{i+1} - \text{h.c.}\right] = \left(\hat{S}\hat{T}\right)^\dagger \hat{H}_{-,\text{hop}}^{\text{OBC}}\left(\frac{\pi}{2},1\right)\left(\hat{S}\hat{T}\right) \\ &= \left(\hat{R}_L\hat{S}\right)^\dagger \hat{H}_{-,\text{hop}}^{\text{OBC}}\left(\frac{\pi}{2},1\right)\left(\hat{R}_L\hat{S}\right).\end{aligned} \tag{3.32}$$

We close this chapter with a concluding remark. Even if the bosonic version of the Anyon-Hubbard model breaks both parity and time-reversal symmetry in general, there are nevertheless specific parameter values where the invariance with respect to a collection of combined discrete symmetries emerge. This could help to classify different states of matter for the bosonic Anyon-Hubbard model, according to their transformation behavior with respect to such discrete symmetry operations. Furthermore as the occurrence of discrete symmetries is of importance in the classification of topological states of matter for non-interacting systems, an analogous classification of the Anyon-Hubbard model would be desirable but lies beyond the scope of this thesis .

# 4 Gutzwiller Mean-Field Theory

In the following part of this thesis we study the mean-field properties of the Anyon-Hubbard model by means of the Gutzwiller variational ansatz. To this end we use here a modified version of the classical Gutzwiller mean-field scheme to calculate quasi-momentum distributions for both the bosonic as well as the anyonic case. We start the discussion by a review of the classical case. In the special case of one-dimensional systems, where quantum fluctuations play a major role [36], mean-field methods can usually not describe the physics of the system quantitatively, as they neglect such fluctuations [37]. Nevertheless they can still be used to gain qualitative insight into physical processes such as phase transitions, which is justified in the following.

## 4.1 Classical Gutzwiller Ansatz

The Gutzwiller ansatz assumes that the true ground state of the system can be decomposed into a product state of different lattice sites, where every local state is approximated by a superposition of number states [2]

$$|\,G\,\rangle = \prod_{i=1}^{L} \left( \sum_{n=0}^{n_{\max}} f_n^i |\,n\,\rangle \right). \tag{4.1}$$

Here $f_n^i$ denote the complex-valued Gutzwiller amplitudes at site $i$ with the corresponding particle number $n$, which represent variational parameters.Furthermore the number state is given by $|\,n\rangle = \frac{(\hat{b}^\dagger)^n}{\sqrt{n!}}\,|\,0\rangle$ and $n_{\max}$ denotes the chosen cut-off, i.e. the maximal allowed occupation number to reduce numerical efforts. Additionally the Gutzwiller amplitudes are subject to the following normalization condition

$$\sum_{n=0}^{n_{\max}} |f_n^i|^2 = 1. \tag{4.2}$$

They are found by extremizing the expectation value of a given Hamiltonian $\langle \hat{H} \rangle$ with respect to the Gutzwiller wave function $|\,G\rangle$. This can be done in different ways, for instance one can assume a given chemical potential $\mu$ as a Lagrange multiplier in a grand canonical approach, or a given mean particle number $n_0 = \langle n \rangle$ per site in a canonical approach. In the following we use the latter canonical approach this leads to a second constrain, that has to be taken into account when minimizing the total energy

$$n_0 = \langle \hat{n} \rangle = \sum_{n=0}^{n_{\max}} |f_n^i|^2 n. \tag{4.3}$$

By fixing a given density per site $n_0 = \langle n \rangle$, the corresponding chemical potential $\mu$ can be derived, after extremalization with respect to the Gutzwiller amplitude $f_n^i$, via

$$\mu = \frac{1}{L} \frac{\partial}{\partial n_0} \langle \hat{H} \rangle. \tag{4.4}$$

Now, in the case of a homogeneous system, one usually assumes that the Gutzwiller amplitudes coincide at every point on the lattice, thus

$$f_n^i \longrightarrow f_n, \tag{4.5}$$

to which we will refer to as the classical Gutzwiller ansatz from here on.
The logic behind the usage of such an restricted ansatz, can be uncovered by considering the limit of a vanishing statistical parameter $\theta$ for (2.30)–(2.33), namely the Bose-Hubbard model. In that case there are only two phases, i.e. the insulating Mott phase as well as the superfluid phase. In both extremal cases the wave function of the system is factorisable, thus one can assume that also in between the two cases the wave function can be approximated by a product form, i.e.

$$\begin{aligned} |\,\text{Mott}\,\rangle &= C \prod_{i=1}^{L} (\hat{b}_i^\dagger)^n |\,0\,\rangle_i \\ |\,\text{Superfluid}\,\rangle &= C \prod_{i=1}^{L} \exp(\sqrt{n}\,\hat{b}_i^\dagger) |\,0\,\rangle_i \end{aligned} \tag{4.6}$$

## 4.2 Modified Gutzwiller Ansatz

In the last chapter we have shown that anyonic systems intrinsically break reflection symmetry. Thus the homogeneity requirement of the classical Gutzwiller ansatz might be too restrictive to describe interesting features of the Anyon-Hubbard model. To overcome that fact, we propose a modified version of the classical Gutzwiller ansatz in the following

$$f_n^j = A_n \exp(ij\beta_n), \tag{4.7}$$

where $A_n \in \mathbb{C}$ and $\beta_n \in \mathbb{R}$. We can rewrite the term (4.6) by using the polar decomposition of complex numbers, leading to

$$f_n^j = A_n \exp(ij\beta_n) = |A_n| \exp(ij\beta_n + \gamma_n), \tag{4.8}$$

where $\gamma_n$ denotes the argument of $A_n$. This ansatz can be interpreted such that we add a linear site-dependent phase term to the Gutzwiller coefficients, while the amplitudes are forced to be equal over the whole lattice. The constraints (4.2)–(4.3), have to be modified in the following way,

$$\sum_{n=0}^{n_{\max}} |f_n^i|^2 = \sum_{n=0}^{n_{\max}} |A_n|^2 = 1, \tag{4.9}$$

$$\langle \hat{n} \rangle = \sum_{n=0}^{n_{max}} |A_n|^2 n. \tag{4.10}$$

Before we apply this new ansatz, we have to show how the expectation value $\langle \hat{O} \rangle$ of the other involved operators can be calculated in detail

$$\langle \hat{b}_j \rangle = \sum_{n=0}^{n_{\max}} f_n^{j*} f_{n+1}^{j} \sqrt{n+1} = \sum_{n=0}^{n_{max}} A_n^* A_{n+1} \exp\left[-ij(\beta_n - \beta_{n+1})\right] \sqrt{n+1} = \langle \hat{b}_j^\dagger \rangle^*, \tag{4.11}$$

$$\begin{aligned} \langle \hat{b}_j^\dagger \exp(i\theta \hat{n}_j) \rangle &= \sum_{n=0}^{n_{max}} A_n^* A_{n+1} \exp\left[-ij(\beta_n - \beta_{n+1})\right] \sqrt{n+1} \exp(i\theta n), \\ &= \langle \exp(-i\theta \hat{n}_j) \hat{b}_j \rangle^* \end{aligned} \tag{4.12}$$

$$\langle \exp(\pm i\theta \hat{n}_j) \rangle = \sum_{n=0}^{n_{max}} |A_n|^2 \exp(\pm i\theta n). \tag{4.13}$$

Now we have to calculate the expectation value of a given Hamiltonian for our new Gutzwiller wave function, and then minimize, for a given set of parameters, with respect to the amplitudes and the phases of the Gutzwiller coefficients. In the following we focus on the following Hamiltonian

$$\hat{H} = \frac{U}{2} \sum_{j=1}^{L} \hat{n}_j \left(\hat{n}_j - 1\right) - J \sum_{j=1}^{L} \left[ \hat{b}_j^\dagger \hat{b}_{j+1} \exp(i\theta \hat{n}_j) + \text{h.c.} \right] - \mu \sum_{j=1}^{L} \hat{n}_j. \tag{4.14}$$

Thus the corresponding expectation value reads

$$\begin{aligned} \langle G | \hat{H} | G \rangle =& \langle G | \frac{U}{2} \sum_{j=1}^{L} \hat{n}_j \left(\hat{n}_j - 1\right) | G \rangle + \langle G | - J \sum_{j=1}^{L} \left[ \hat{b}_j^\dagger \hat{b}_{j+1} \exp(i\theta \hat{n}_j) + \text{h.c.} \right] | G \rangle \\ &+ \langle G | - \mu \sum_{j=1}^{L} \hat{n}_j | G \rangle. \end{aligned} \tag{4.15}$$

Here we remark that (4.12) corresponds to the Hamiltonian $\hat{H}_-^{PBC}$ in equation (2.32), when the boundary term from site $L$ to the site $L+1$ is dropped, and periodic boundary conditions are assumed. We do that, to compare our results to the literature, where the term is usually neglected. Furthermore the boundary term will scale like $\frac{1}{L}$, thus it will drop out in the thermodynamic limit.
Now we calculate every expectation value separately

$$\epsilon_\mu = \langle G | - \mu \sum_{j=1}^{L} \hat{n}_j | G \rangle = -\mu \langle \hat{N} \rangle = -\mu L \sum_{n=0}^{n_{max}} |A_n|^2 n, \tag{4.16}$$

$$\epsilon_U = \langle G | \frac{U}{2} \sum_{j=1}^{L} \hat{n}_j \left(\hat{n}_j - 1\right) | G \rangle = \frac{U}{2} L \sum_{n=0}^{n_{\max}} |A_n|^2 n(n-1), \tag{4.17}$$

$$\epsilon_J = \langle G | - J \sum_{j=1}^{L} \left[ \hat{b}_j^\dagger \hat{b}_{j+1} \exp(i\theta \hat{n}_j) + \text{h.c.} \right] | G \rangle,$$

$$= -J \sum_{j=1}^{L} \sum_{n,m}^{n_{\max}} \sqrt{(n+1)(m+1)} [A_n \exp(ij\beta_n) A_{n+1}^* \exp(-ij\beta_{n+1}) A_m^* \exp(-i(j+1)\beta_m) \quad (4.18)$$
$$A_{m+1} \exp(i(j+1)\beta_{m+1}) \exp(i\theta n) + \text{c.c.}].$$

Now in order to numerically solve the extremalization problem, we need to fix a cut-off for the maximal occupation $n_{\max}$. It should be chosen in such a way that the physics is adequately captured, while neglecting high-energy degrees of freedom. The kind of cut-off we discuss in the following is the hard-core case $n_{\max} = 1$, as well as the soft-core case $n_{\max} = 2$.

## 4.3 Hard-Core Case

In the hard-core case, only single occupancy is allowed, thus the particles locally behave like fermions. This restriction leads to the following auxiliary constraints on the variational wave function (4.8)–(4.9)

$$|A_0|^2 + |A_1|^2 = 1, \quad (4.19)$$
$$n_0 = |A_1|^2. \quad (4.20)$$

Thus the expectation values (4.14)–(4.16) are given by

$$\epsilon_\mu = -\mu L n_0, \quad (4.21)$$

$$\epsilon_U = 0, \quad (4.22)$$

$$\epsilon_J = -J \sum_{j=1}^{L} \left[ |A_0|^2 |A_1|^2 \exp\left[-i(\beta_0 - \beta_1)\right] + \text{c.c.} \right] = -2JLn_0(1-n_0)\cos(\Delta\beta_0), \quad (4.23)$$

where we have already inserted the auxiliary conditions, and we used the abbreviation $\Delta\beta_0 = \beta_0 - \beta_1$.
One can already see the consequences of the hard-core condition, namely the vanishing of the on-site interaction term (4.16), as well as the absence of any $\theta$-dependence. This can be already explained at the level of the Hamiltonian (4.12), if we restrict the dimension of the local Hilbert-space to two. Then the Hamiltonian can be written as

$$\hat{H} = -J \sum_{j=1}^{L} \left( \hat{b}_j^\dagger \hat{b}_{j+1} + \text{h.c.} \right) - \mu \sum_{j=1}^{L} \hat{n}_j, \quad (4.24)$$

where the vanishing of the interaction term as well as the exponential comes out of the fermion-like condition $(\hat{b}^\dagger)^2 = 0$.
Now we have to minimize the total Gutzwiller energy per lattice site with respect to the remaining parameter $\Delta\beta_0$

$$\min[E_{\text{tot}}/L] = \min[-2Jn_0(1-n_0)\cos(\Delta\beta_0) - \mu n_0], \tag{4.25}$$

which leads to $\Delta\beta_0 = 2\pi k$ with $k \in \mathbb{Z}$. This gives the same result as the classical Gutzwiller ansatz. As the hard-core case was already discussed in the literature [2], we will focus in the following on the soft-core case.

## 4.4 Soft-Core Case

In the soft-core case neither the interaction term nor the density-dependent Peierls phase vanish, thus the impact of the statistical parameter on the ground-state as well as on the correlation functions can be studied in this case. The auxiliary conditions (4.8)–(4.9) in this case are given by

$$|A_0|^2 + |A_1|^2 + |A_2|^2 = 1, \tag{4.26}$$

$$|A_1|^2 + 2|A_2|^2 = n_0. \tag{4.27}$$

Furthermore the expectation values for the chemical potential as well the interaction term (4.14)–(4.15) read in this case

$$\epsilon_\mu = -\mu L(|A_1|^2 + 2|A_2|^2) = -\mu L n_0, \tag{4.28}$$

$$\epsilon_U = LU|A_2|^2. \tag{4.29}$$

As the expectation value for the kinetic energy (4.10) shows the first non-trivial features, we will calculate it in detail

$$\begin{aligned}\epsilon_J = &- J\sum_{j=1}^{L}\Big(\big\{|A_0|^2|A_1|^2\exp[-i(\beta_0-\beta_1)] + \text{c.c.}\big\} + \big\{2|A_1|^2|A_2|^2\exp[-i(\beta_1-\beta_2-\theta)] + \text{c.c.}\big\} \\ &+ \sqrt{2}\,\big\{A_1^{2*}A_0A_2\exp[ij(\beta_0+\beta_2-2\beta_1)]\exp[-i(\beta_1+\beta_2)] + \text{c.c.}\big\} \\ &+ \sqrt{2}\,\big\{A_1^2A_0^*A_2^*\exp[-ij(\beta_0+\beta_2-2\beta_1)]\exp[-i(\beta_0+\beta_1-\theta)] + \text{c.c.}\big\}\Big).\end{aligned} \tag{4.30}$$

As a consequence the expectation value is still site-dependent, so we have to calculate the sum over the whole lattice. The problem is now that the energy (4.14) should be extensive in the thermodynamic limit. We observe that the $j$-dependence of the kinetic energy (4.30) has the form of a geometric sum. Thus we have to demand $\sum_{j=1}^{L} q^j = L$ for every $j$-dependent term. This leads to the following restrictions for the phases

$$\beta_0 + \beta_2 - 2\beta_1 = 2\pi k, \;\; k \in \mathbb{Z}. \tag{4.31}$$

Furthermore we can express all phases by their differences, and then eliminate one of them

$$\Delta\beta_0 = 2\pi k + \Delta\beta_1, \tag{4.32}$$

with $\Delta\beta_0 = \beta_0 - \beta_1$ and $\Delta\beta_1 = \beta_1 - \beta_2$. Additionally we use the polar decomposition of the Gutzwiller coefficients $A_n = |A_n|\exp(i\gamma_n)$, which leads to the following expression for the expectation value for the kinetic energy

$$\begin{aligned}\epsilon_J/L = -J|A_1|^2 \left[2|A_0|^2\cos(\Delta\beta_0) + 4|A_2|^2\cos\left(\Delta\beta_0 - \theta\right)\right. \\ \left. +4\sqrt{2}\,|A_0||A_1|\cos\left(\Delta\beta_0 - \frac{\theta}{2}\right)\cos\left(\Delta\gamma - \frac{\theta}{2}\right)\right],\end{aligned} \tag{4.33}$$

where $\Delta\gamma = \gamma_0 + \gamma_2 - 2\gamma_1$ denotes the differences of the classical Gutzwiller phases. If the additional phases would be chosen such that $\Delta\beta_0 = 2\pi f$ with $f \in \mathbb{Z}$, we would recover again the classical Gutzwiller case.
The full energy per lattice site is given by

$$\begin{aligned}E_{\text{tot}}/L = -J|A_1|^2 \left[2|A_0|^2\cos(\Delta\beta_0) + 4|A_2|^2\cos(\Delta\beta_0 - \theta) + \right. \\ \left. 4\sqrt{2}\,|A_0||A_1|\cos\left(\Delta\beta_0 - \frac{\theta}{2}\right)\cos\left(\Delta\gamma - \frac{\theta}{2}\right)\right] - \mu n_0 + U|A_2|^2.\end{aligned} \tag{4.34}$$

We choose

$$\Delta\gamma = 2\pi l + \frac{\theta}{2} \quad \text{with} \quad l \in \mathbb{Z}, \tag{4.35}$$

as this minimizes the classical Gutzwiller energy. The next step is now to extremize the total energy with respect to the Gutzwiller amplitudes and phases, for a given set of parameters. In the following we assume, that the amplitudes and phases are independent variables, and we extremize first with respect to $\Delta\beta_0$. Thus we have to calculate

$$\frac{\partial}{\partial\Delta\beta_0} E_{\text{tot}}/L = 0 \tag{4.36}$$

This leads, after some lengthy but straight-forward algebra, to the phase difference which minimizes the total energy

$$\Delta\beta_0 = \arctan\left[\frac{2|A_2|\left\{|A_2|\sin(\theta) + |A_0||A_2|\sqrt{2}\sin(\frac{\theta}{2})\right\}}{|A_0|^2 + 2|A_2|^2\cos(\theta) + 2\sqrt{2}\,|A_0||A_2|\cos(\frac{\theta}{2})}\right]. \tag{4.37}$$

The amplitudes of the Gutzwiller coefficients cannot be evaluated analytically. Thus we have to minimize them numerically, where the constraints (4.26)–(4.27) have to be fulfilled This was done with a standard Mathematica package.

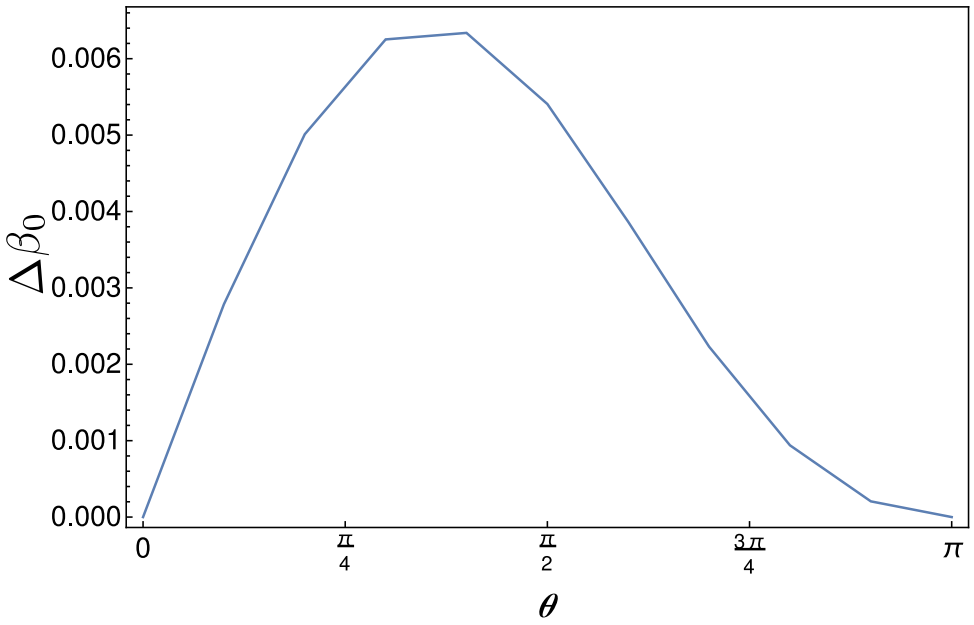


**FIG. 4.1:** Phase difference $\Delta\beta_0$ in units of $J$ for density $n_0 = 0.25$ and $\frac{U}{J} = 10$ and system length $L = 100$.

### 4.4.1 Energy

In order to calculate the energy of the Gutzwiller ansatz, we have to reinsert the expression (4.37) for $\Delta\beta_0$ in the Gutzwiller energy (4.34). After some algebraic manipulations it turns out that this expression is equivalent to the classical Gutzwiller energy.

$$\begin{aligned} E_{tot}/L = &- J|A_1|^2 \left[2|A_0|^2 + 4|A_2|^2\cos(\theta) + 4\sqrt{2}|A_0||A_1|\cos\left(\frac{\theta}{2}\right)\right] \\ &- \mu n_0 + U|A_2|^2. \end{aligned} \tag{4.38}$$

Thus from this point of view the modified ansatz is not superior to the classical Gutzwiller case. Nevertheless the improvement of the modified ansatz is justified in the next subsection. Additionally in Ref . [2], it is claimed that their ansatz is superior to the classical, as the energy they have obtained acts as a lower bound for the standard case. Nevertheless their energy is not dependent on the statistical parameter $\theta$, which contradicts to the data obtained from the DMRG in private communication with K. Jägering [38] (FIG. 4.3). Also from a heuristical point of view this can not be true, as we except a rise of the energy as the pseudo-fermionic limit is approached, due to some kind of Pauli-repulsion, which is explained by a weak coupling analysis in [39]. The variational energy should not only be minimal, but also should not contradict to the physical properties of the system. Thus we argue, that in that sense, the classical Gutzwiller ansatz is superior to the one obtained in [2] as it describes the growth of energy with increasing $\theta$ correctly (FIG. 4.4). In the extremalization process a small density was chosen $n_0 = 0.1$, as the obtained energy is not only qualitatively close to the DMRG-data but also quantitatively. This originates from the fact that in the dilute limit the interaction strength $U$ plays a less dominant role and the assumption of a factorisable wave-function is more appropriate, i.e. quantum fluctuations play a subordinate role.

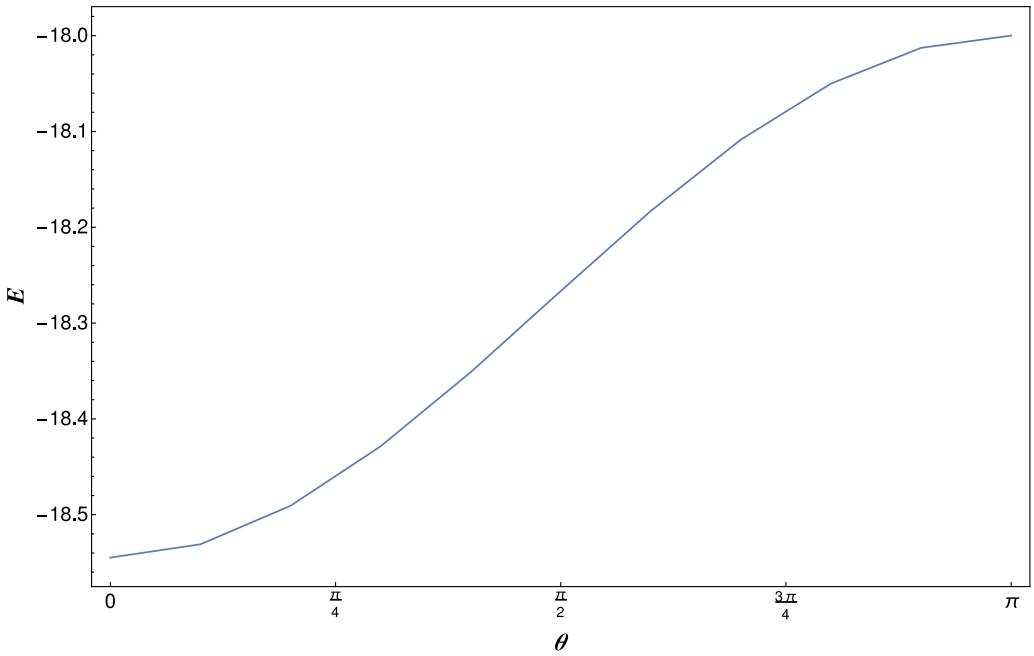


**FIG. 4.2:** Classical Gutzwiller energy in units of $J$ as function of the statistical parameter $\theta$ for density $n_0 = 0.1$ and $\frac{U}{J} = 10$ and system length $L = 100$.

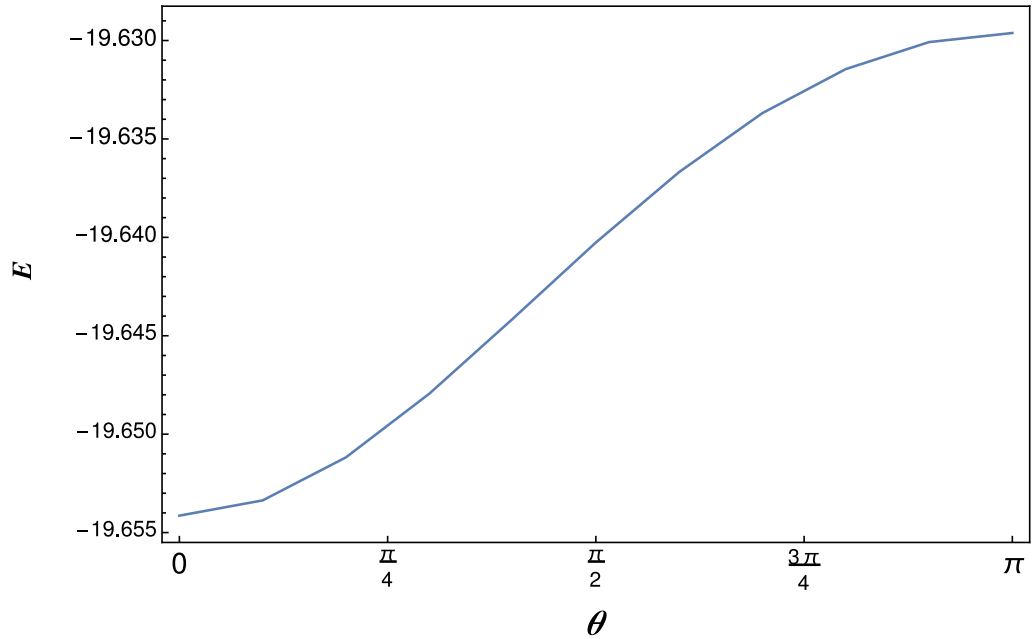


**FIG. 4.3:** Energy in units of $J$ as function of the statistical parameter $\theta$ for density $n_0 = 0.1$ and $\frac{U}{J} = 10$ and system length $L = 100$, obtained by DMRG in private communication with K. Jägering [38].

### 4.4.2 Quasi-Momentum Distributions Of Bosons

In this subsection we will calculate the pair-correlation function of bosons in the Gutzwiller-approximation, for the case $n_{\max} = 2$. As the Fourier transformed pair-correlation function can be measured via time-of-flight measurements, they might provide a valuable theoretic description of the corresponding observables in the laboratory. The pair-correlation function in the Gutzwiller frame is given by

$$\begin{aligned}\langle G \mid \hat{b}_i^\dagger \hat{b}_j \mid G\rangle &= \delta_{ij}\langle G \mid \hat{n}_i \mid G\rangle + (1-\delta_{ij})\langle G \mid \hat{b}_i^\dagger \mid G\rangle\langle G \mid \hat{b}_j \mid G\rangle \\ &= \delta_{ij} n_0 + (1-\delta_{ij})\langle \hat{b}_i^\dagger\rangle\langle \hat{b}_j\rangle,\end{aligned} \tag{4.39}$$

where we used just the constraint of a fixed density, and a short-hand notation of the expectation value in the second line. If we use now the definition of the expectation values for the involved operators (4.9) within the modified Gutzwiller ansatz, it follows

$$\begin{aligned}\langle \hat{b}_i^\dagger \hat{b}_j\rangle = \delta_{ij} n_0 + (1-\delta_{ij}) &\sum_{n=0}^{n_{\max}} A_n A_{n+1}^* \exp\left[ij(\beta_n - \beta_{n+1})\right]\sqrt{n+1} \\ &\times \sum_{m=0}^{m_{\max}} A_m^* A_{m+1} \exp\left[-ii(\beta_m - \beta_{m+1})\right]\sqrt{m+1}.\end{aligned} \tag{4.40}$$

In the next step we fix the cut-off to $n_{\max} = 2$ and use again the polar decomposition for the Gutzwiller coefficients, as well as the relation (4.32)

$$\begin{aligned}\langle \hat{b}_i^\dagger \hat{b}_j\rangle = \delta_{ij} n_0 + (1-\delta_{ij}) &\left(|A_1|\left\{|A_0|\exp\left[i(\gamma_0-\gamma_1)\right] + \sqrt{2}|A_2|\exp\left[i(\gamma_1-\gamma_2)\right]\right\}\right) \\ \times |A_1|&\left\{|A_0|\exp\left[-i(\gamma_0-\gamma_1)\right] + \sqrt{2}|A_2|\exp\left[-i(\gamma_1-\gamma_2)\right]\exp\left[i(i-j)\Delta\beta_0\right]\right\}\end{aligned} \tag{4.41}$$

This can be further simplified to,

$$\langle \hat{b}_i^\dagger \hat{b}_j\rangle = \delta_{ij} n_0 + (1-\delta_{ij})|A_1|^2\left\{|A_0|^2 + 2\sqrt{2}|A_0||A_2|\cos(\Delta\gamma) + 2|A_2|^2\exp\left[i(i-j)\Delta\beta_0\right]\right\}. \tag{4.42}$$

We can already see at this point, that the pair-correlation depends only on the spatial distance of the two given sites, which is a general property of translationally invariant systems. Additionally, if we would set $\Delta\beta_0 = 2\pi f$ with $f \in \mathbb{Z}$, we would recover the classical Gutzwiller ansatz which does not provide any spatial dependence of the pair-correlation function.

As we are interested in the quasi-momentum distribution we have to Fourier-transform Eq. (4.36),

$$\langle \hat{n}_k^b\rangle = \frac{1}{L}\sum_{i,j=1}^{L} \exp\left[ik(i-j)\right]\langle \hat{b}_i^\dagger \hat{b}_j\rangle. \tag{4.43}$$

In (4.37) the lattice spacing is set to unity and the quasi-momentum k runs from $\frac{2\pi}{L}$ to $2\pi$. Now we can calculate the quasi-momentum distribution by inserting (4.42) in (4.43),

$$\langle \hat{n}_k^b\rangle = \frac{1}{L}\sum_{i,j=1}^{L} \exp\left[i(k+\Delta\beta_0)(i-j)\right]\left\{\delta_{ij} n_0 + (1-\delta_{ij})|A_1|^2\left[|A_0|^2 + 2\sqrt{2}|A_0||A_2|\cos(\Delta\gamma) + 2|A_2|^2\right]\right\}$$

$$= n_0 - |A_1|^2 \left[ |A_0|^2 + 2\sqrt{2}|A_0||A_2|\cos\left(\frac{\theta}{2}\right) + 2|A_2|^2 \right]$$
$$+\frac{1}{L}|A_1|^2 \left[ |A_0|^2 + 2\sqrt{2}|A_0||A_2|\cos\left(\frac{\theta}{2}\right) + 2|A_2|^2 \right] \frac{1-\cos\left[(k+\Delta\beta_0)L\right]}{1-\cos\left[k+\Delta\beta_0\right]}. \tag{4.44}$$

In the next step we evaluate the thermodynamic limit, L $\to \infty$, and get

$$\langle \hat{n}_k^b \rangle_{L\to\infty} = n_0 - |A_1|^2 \left[ |A_0|^2 + 2\sqrt{2}|A_0||A_2|\cos\left(\frac{\theta}{2}\right) + 2|A_2|^2 \right] \tag{4.45}$$
$$+|A_1|^2 \left[ |A_0|^2 + 2\sqrt{2}|A_0||A_2|\cos\left(\frac{\theta}{2}\right) + 2|A_2|^2 \right] \delta(k+\Delta\beta_0).$$

Ordinary bosons condense at $k = 0$, whereas in our case the correlated hopping induces a shift and the particles condense at $k = -\Delta\beta_0$. This can be interpreted as a manifestation of the broken parity or time reversal symmetry discussed earlier.
Before we show the plots for Eq. (4.38) we discuss some special cases for $\Delta\beta_0$ in (4.37), for different densities, as well as different values of $\theta$. $\Delta\beta_0(\theta, |A_0|, |A_2|)$ is a function of $\theta$ as well as the Gutzwiller amplitudes $|A_i|$, which correspond to different density regimes. That means if $n_0 \ll 1$, then $|A_2| \approx 0$ and if $n_0$ is large, then $|A_0| \approx 0$. Thus we obtain,

$$\Delta\beta_0(0, |A_0|, |A_2|) = \arctan(0) = 0 = \Delta\beta_0(\theta, |A_0|, 0) \tag{4.46}$$

$$\Delta\beta_0(\theta, 0, |A_2|) = \arctan\left[\frac{\sin(\theta)}{\cos(\theta)}\right] = \arctan\left[\tan(\theta)\right] = \theta. \tag{4.47}$$

Now the LHS of (4.46) can be interpreted such that, for $\theta = 0$ which corresponds to the Bose-Hubbard Hamiltonian, the particles behave like ordinary bosons and thus condense at $k \approx 0$. The RHS of (4.46) simply states, that this is also true for very low densities (FIG. 4.4). Whereas eq. (4.47) shows that in the high density regime, the particles condense at $k \approx -\theta$ (FIG. 4.9)
.

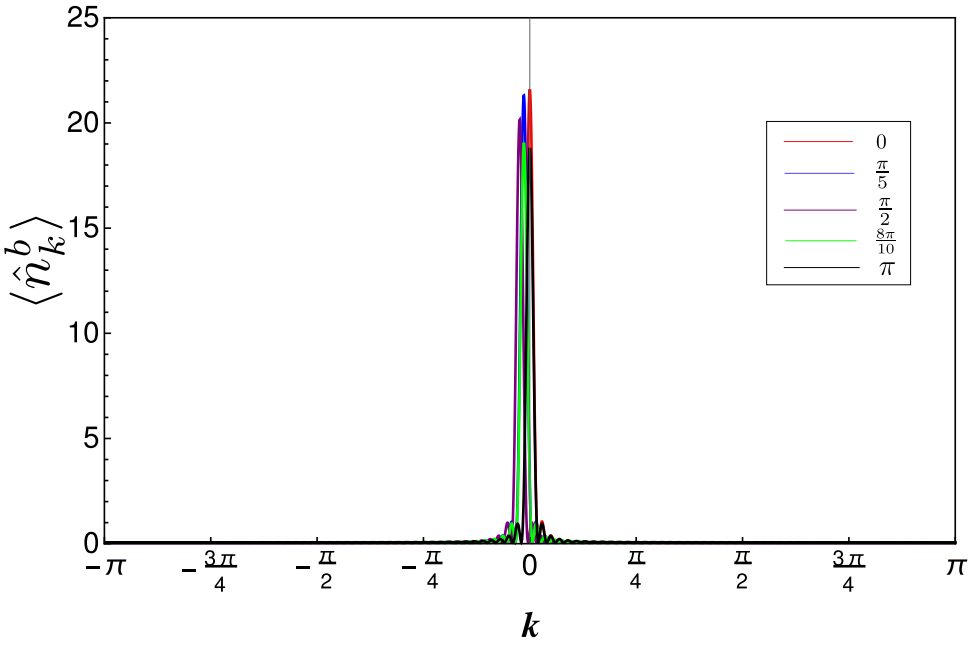


**FIG. 4.4:** Quasi-momentum distribution $\langle \hat{n}_k^b \rangle$ for density $n_0 = 0.25$ and $\frac{U}{J} = 10$, system length $L = 100$ and different values of $\theta$.

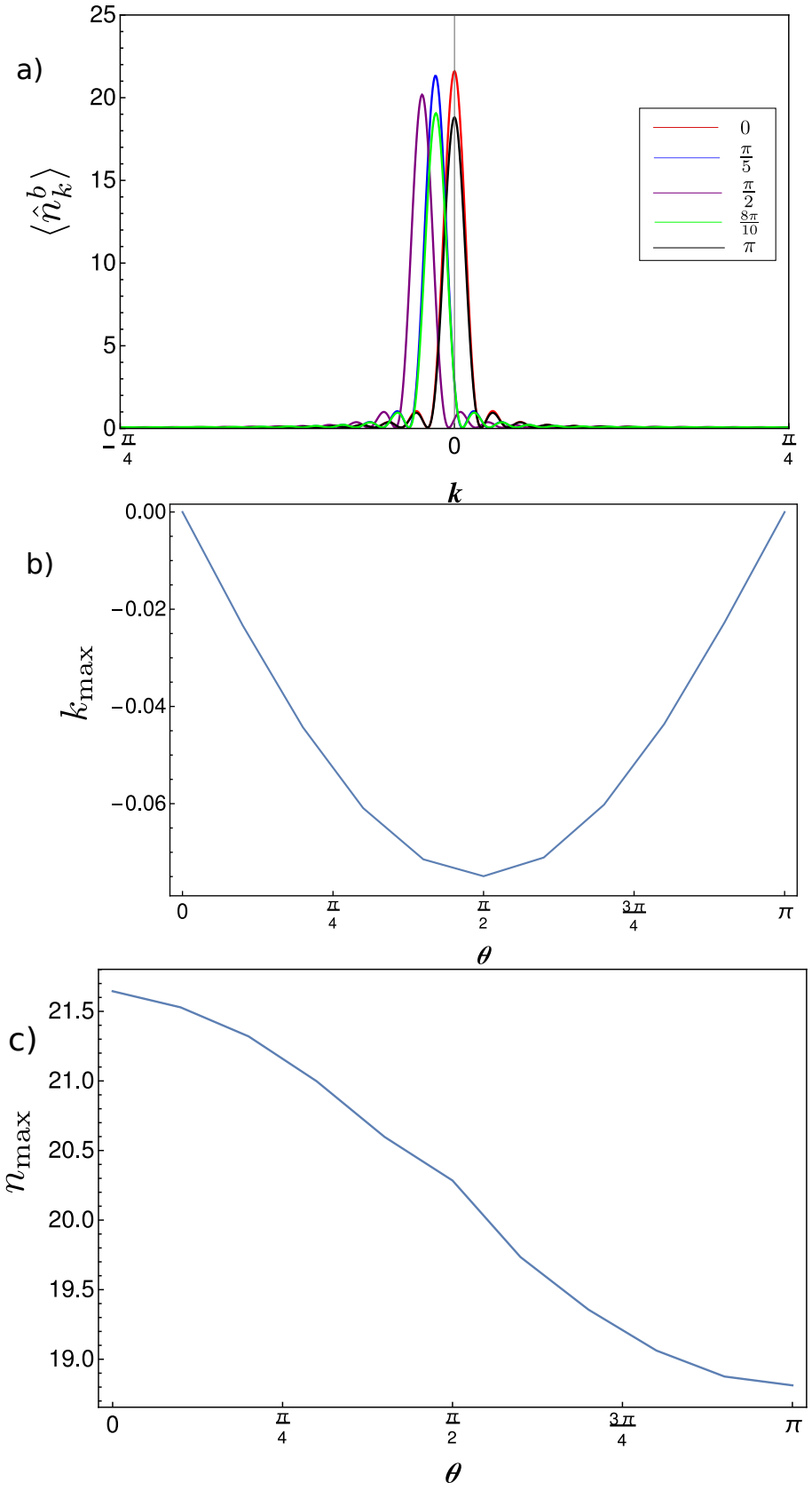


**FIG. 4.5:** a) Zoom of FIG.4.3 of quasi-momentum distribution $\langle \hat{n}_k^b \rangle$, b) momentum value $k_{\max}$ where $\langle \hat{n}_k^b \rangle$ attains its maximum, c) value of $\langle \hat{n}_k^b \rangle$ at the maximum $n_{\max}$, for density $n_0 = 0.25$ and $\frac{U}{J} = 10$, system length $L = 100$ and different values of $\theta$

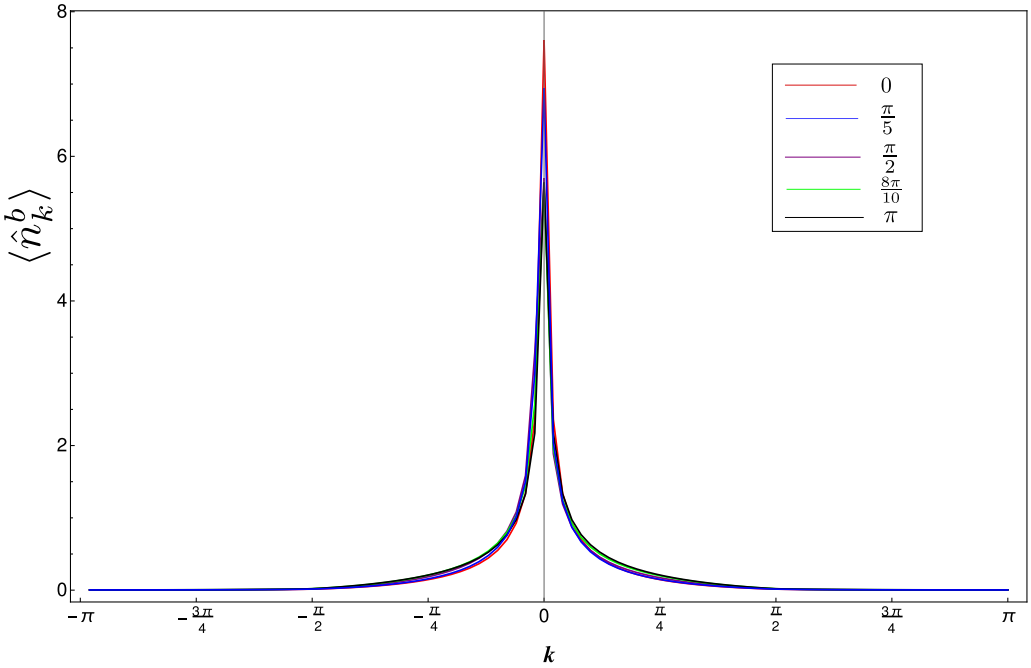


**FIG. 4.6:** DMRG-data of $\langle \hat{n}_k^b \rangle$, for density $n_0 = 0.25$, $\frac{U}{J} = 10$, system length $L = 100$ and different values of $\theta$ [38].

Comparing the Gutzwiller results with the DMRG-data it turns out that they coincide qualitatively, whereas they differ quantitatively. This quantitative difference can be explained by the general inadequacy of mean-field approaches in low-dimensional systems. Also all quasi-momentum distributions obtained by the DMRG are broader than their Gutzwiller pendant, this originates from the fact that mean-field calculations neglect quantum-fluctuations which usually broaden the distribution [2]. For low densities (FIG. 4.4, FIG. 4.6) the momentum-shift is negligible, this can be explained by the vanishing of the phase term (4.24) in the hard-core limit. The momentum-shift becomes larger for higher densities but is still small for densities below unit filling (FIG. 4.8 a, FIG. 4.7). Whereas above unit filling the particles condense roughly at $k \approx -\theta$ (FIG. 4.9 a, FIG. 4.10), as explained in Eq. (4.47).
In (FIG. 4.5 b), it can be seen that the momentum values where the quasi-momentum-distribution attains it's maximum, is a parabolic function of the statistical parameter $\theta$, centered around $\theta = \frac{\pi}{2}$. In the case of (FIG. 4.7 b) the center of the function $k_{\max}(\theta)$ is shifted to smaller $\theta$-values, but the parabolic form remains intact. In contrast to that in (FIG. 4.9 b) the parabolic form is lost and $k_{\max}(\theta)$ is linearly decreasing with $\theta$. The parabolic form implies an invariance of $k_{\max}(\theta)$ with respect to $\theta \longrightarrow -\theta$ around $\theta = \frac{\pi}{2}$. The inversion of $\theta \longrightarrow -\theta$ on the level of the Hamiltonian (4.13) has the same effect as a time reversal transformation, i.e. a complex conjugation. Additionally we showed in chapter 3.2 that for some densities and $\theta$-values there might be emerging discrete symmetries, for example a combined local U(1) and time-reversal invariance. Thus the parabolic shape of $k_{\max}(\theta)$ in (FIG. 4.5 b, FIG. 4.7 b) might be a signature for that kind of additional symmetry, while the linear behavior in (FIG. 4.9 b) might denote its vanishing.
The maximal value of the quasi-momentum-distribution $n_{\max}(\theta)$ is always monotonically decreasing with $\theta$ for all calculated density regimes, and does not drastically changes it's basic shape (FIG. 4.5 c, FIG. 4.8 c, FIG. 4.9 c). We interpret this decreasing with growing $\theta$ as the

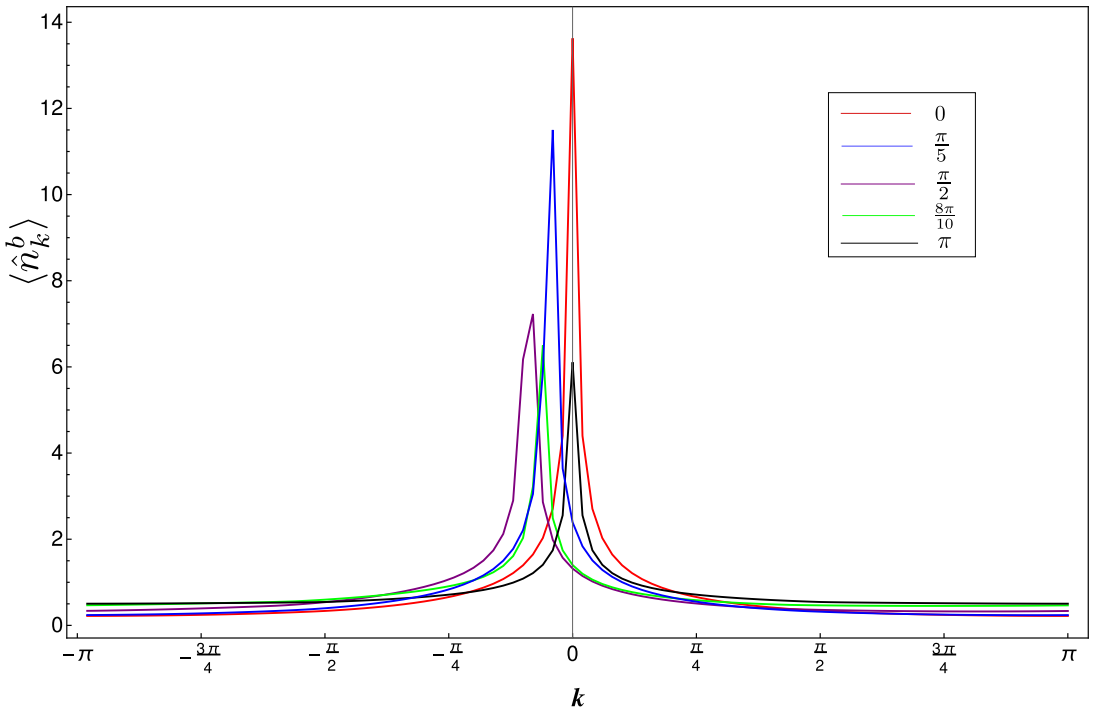


**FIG. 4.7:** DMRG-data of $\langle \hat{n}_k^b \rangle$, for density $n_0 = 0.75$, $\frac{U}{J} = 10$, system length $L = 100$ and different values of $\theta$ [38].

presence of an effective interaction induced by the increasing anti-symmetrization of the non-local commutators [22]. This effect seems to be weaker for low densities in comparison to higher ones. This stems from the fact that in the low density regime neighbouring sites are more likely to be unpopulated an thus the effect is not very pronounced.

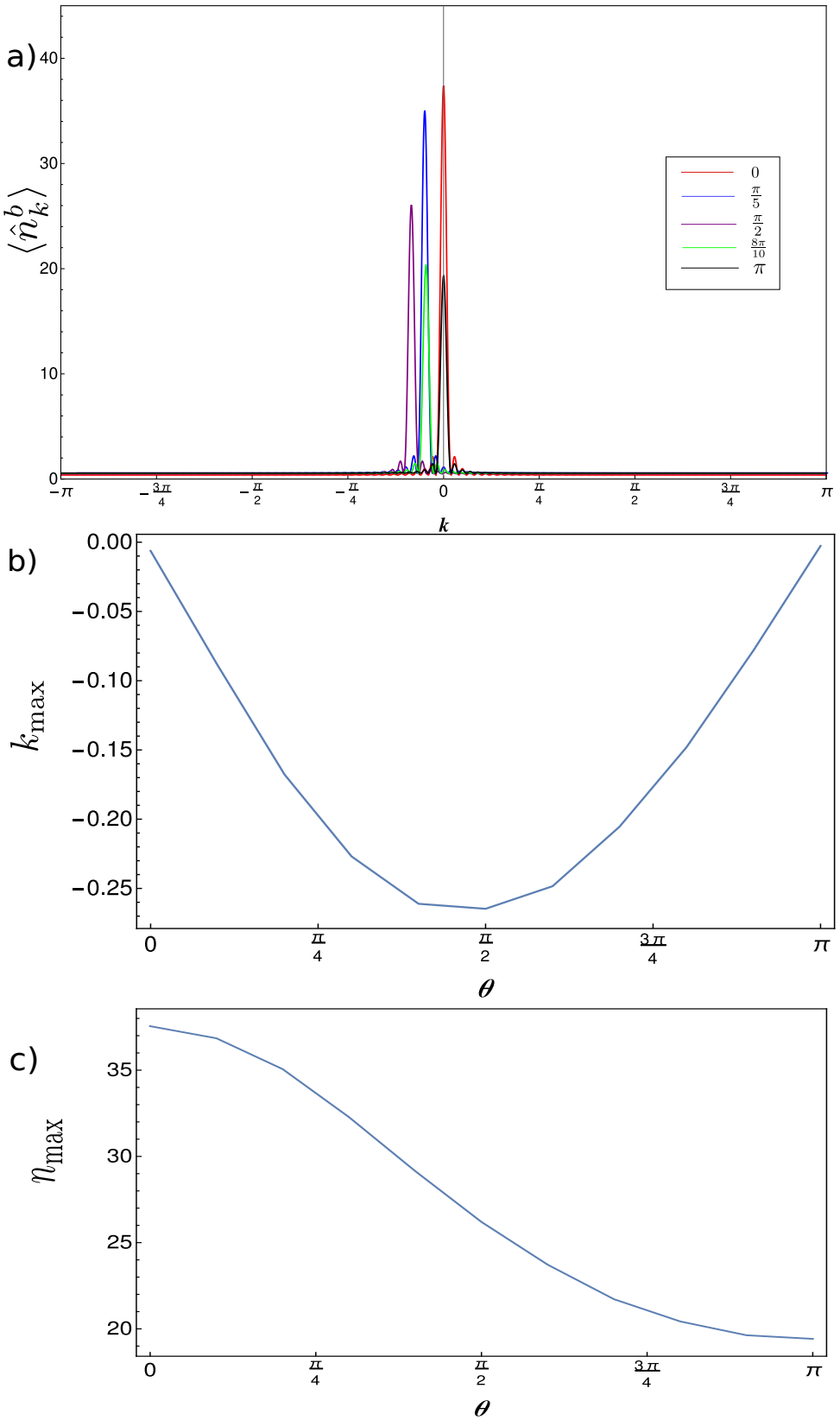


**FIG. 4.8:** a) Quasi-momentum distribution $\langle \hat{n}_k^b \rangle$, b) momentum value $k_{\max}$ where $\langle \hat{n}_k^b \rangle$ attains its maximum, c) value of $\langle \hat{n}_k^b \rangle$ at the maximum $n_{\max}$, for density $n_0 = 0.75$ and $\frac{U}{J} = 10$, system length $L = 100$ and different values of $\theta$

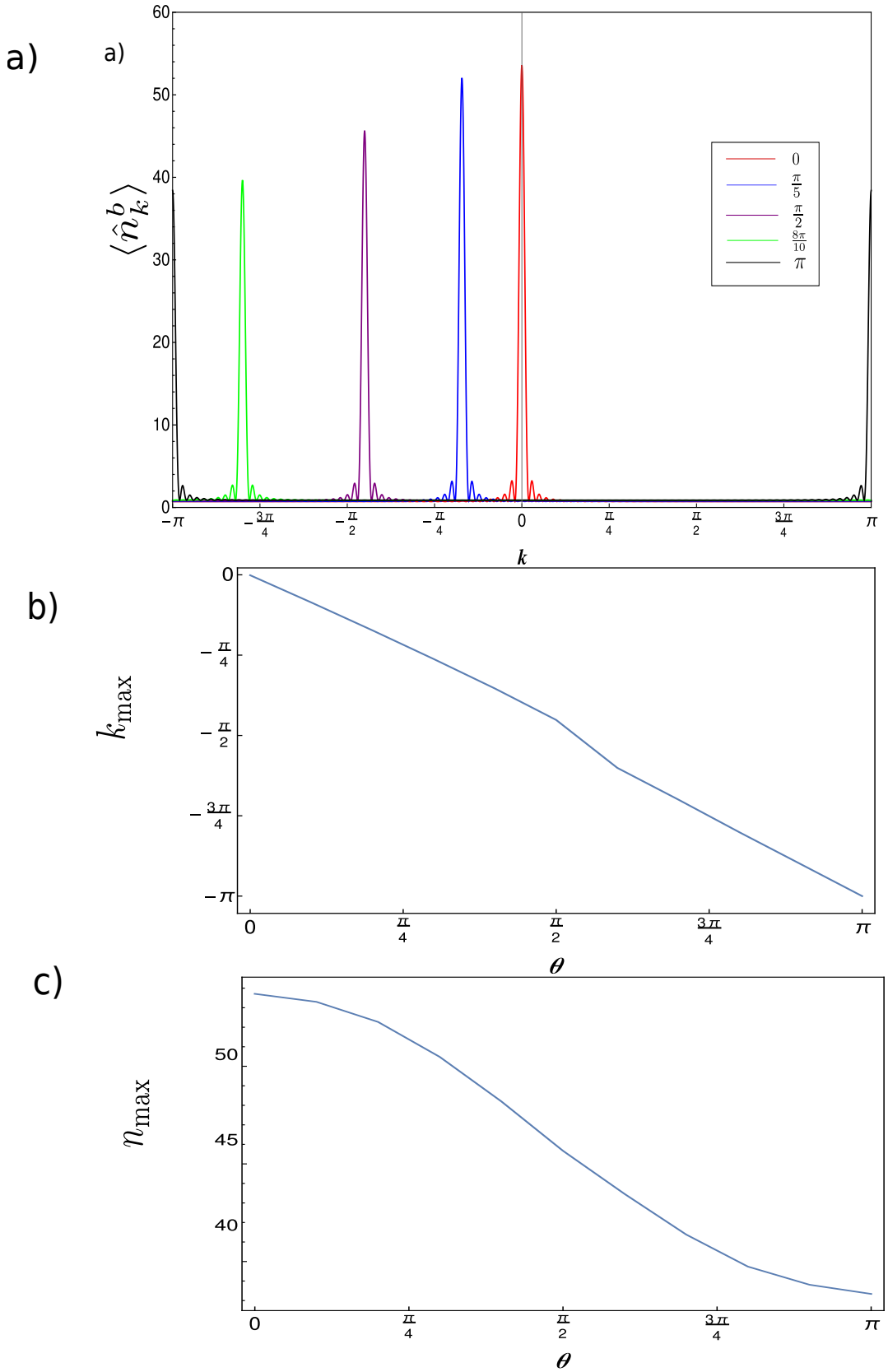


**FIG. 4.9:** a) Quasi-momentum distribution $\langle \hat{n}_k^b \rangle$, b) momentum value $k_{\max}$ where $\langle \hat{n}_k^b \rangle$ attains its maximum, c) value of $\langle \hat{n}_k^b \rangle$ at the maximum $n_{\max}$, for density $n_0 = 1.25$ and $\frac{U}{J} = 10$, system length $L = 100$ and different values of $\theta$

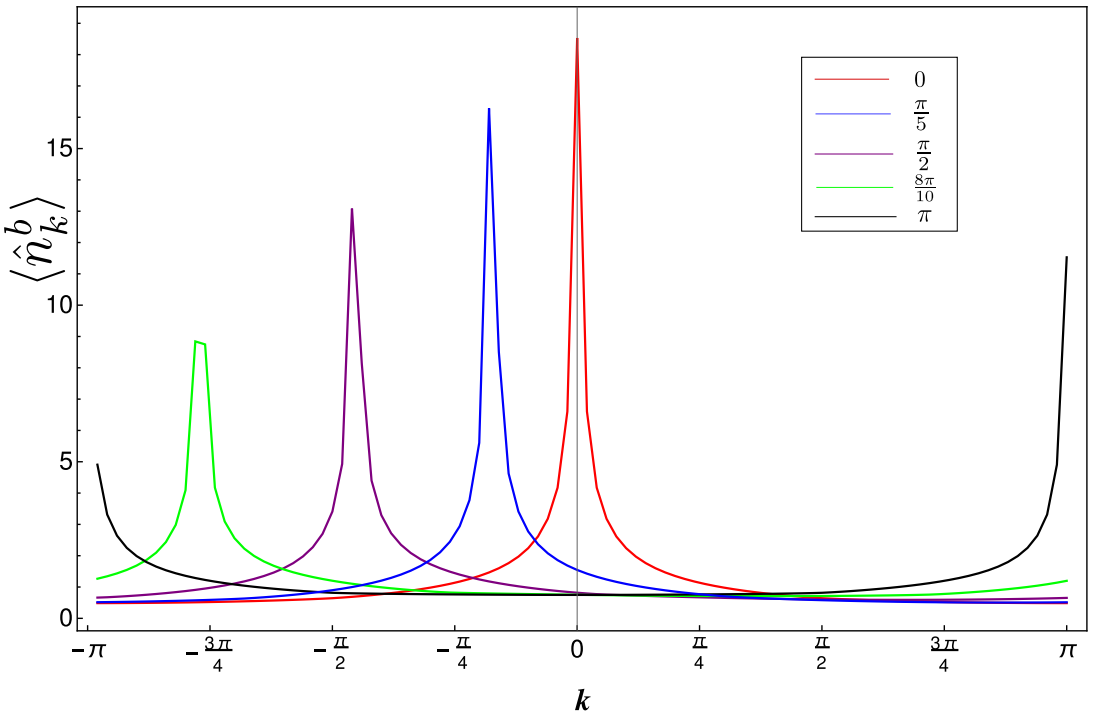


**FIG. 4.10:** DMRG-data of $\langle \hat{n}_k^b \rangle$, for density $n_0 = 1.25$, $\frac{U}{J} = 10$, system length $L = 100$ and different values of $\theta$ [38].

### 4.4.3 Quasi-Momentum Distributions Of Anyons

The same procedure as in subsection 4.4.2 can also be performed for the anyonic pair-correlation function. Although it is not clear if this quantity is an observable in an experiment, a theoretical explanation is nevertheless eligible. As anyons are defined to be bosons, attached with the non-local Jordan-Wigner string, the order of the involved spatial indices is important, in contrast to the purely bosonic case. Thus if we have two spatial indices $i$ and $j$, we have to consider the cases $i = j$, $i > j$ and $i < j$ separately in our calculation. For the case $i = j$ the pair correlation function of anyons is given by

$$\langle \hat{a}_i^\dagger \hat{a}_j \rangle = \delta_{ij} n_0, \tag{4.48}$$

but in the case of $i < j$ we get

$$\begin{aligned} \langle \hat{a}_i^\dagger \hat{a}_j \rangle^{i<j} = \langle \hat{b}_i^\dagger \hat{K}_{-,i}^\dagger \hat{K}_{-,j} \hat{b}_j \rangle = \langle \hat{b}_i^\dagger \exp(i\theta \sum_{x=i}^{j-1} \hat{n}_x) \hat{b}_j \rangle = \langle \hat{b}_i^\dagger \prod_{x=i}^{j-1} \exp(i\theta \hat{n}_x) \hat{b}_j \rangle \\ = \langle \hat{b}_i^\dagger \exp(i\theta \hat{n}_i) \rangle \prod_{x=i+1}^{j-1} \langle \exp(i\theta \hat{n}_x) \rangle \langle \hat{b}_j \rangle. \end{aligned} \tag{4.49}$$

The case $i > j$ can be evaluated analogously,

$$\langle \hat{a}_i^\dagger \hat{a}_j \rangle^{i>j} = \langle \hat{b}_i^\dagger \hat{K}_{-,i}^\dagger \hat{K}_{-,j} \hat{b}_j \rangle = \langle \hat{b}_i^\dagger \exp(-i\theta \sum_{x=j}^{i-1} \hat{n}_x) \hat{b}_j \rangle = \langle \hat{b}_i^\dagger \prod_{x=j}^{i-1} \exp(-i\theta \hat{n}_x) \hat{b}_j \rangle \\ = \langle \hat{b}_i^\dagger \rangle \prod_{x=j+1}^{i-1} \langle \exp(-i\theta \hat{n}_x) \rangle \langle \exp(-i\theta \hat{n}_j) \hat{b}_j \rangle. \tag{4.50}$$

Now we have to form the expectation value with respect to the Gutzwiller wave function, and restrict the maximal occupancy to $n_{\max} = 2$

$$\langle \hat{a}_i^\dagger \hat{a}_j \rangle^{i<j} = |A_1|^2 \left( |A_0|^2 + \sqrt{2} |A_0||A_2| \left\{ \exp\left[ i\Delta\gamma \right] + \exp\left[ -i(\Delta\gamma - \theta) \right] \right\} + 2|A_2|^2 \exp\left[ i\theta \right] \right) \\ \times \left\{ |A_0|^2 + |A_1|^2 \exp\left[ i\theta \right] + |A_2|^2 \exp\left[ 2i\theta \right] \right\}^{j-i-1} \exp\left[ i(i-j)\Delta\beta_0 \right]. \tag{4.51}$$

For this result we introduce the following short-hand notation

$$\langle \hat{a}_i^\dagger \hat{a}_j \rangle^{i<j} = \frac{C}{z} \left[ \frac{\exp(i\Delta\beta_0)}{z} \right]^{i-j}, \tag{4.52}$$

with

$$C = |A_1|^2 \left( |A_0|^2 + \sqrt{2} |A_0||A_2| \left\{ \exp\left[ i\Delta\gamma \right] + \exp\left[ -i(\Delta\gamma - \theta) \right] \right\} + 2|A_2|^2 \exp\left[ i\theta \right] \right) \tag{4.53}$$

$$z = \left\{ |A_0|^2 + |A_1|^2 \exp\left[ i\theta \right] + |A_2|^2 \exp\left[ 2i\theta \right] \right\}. \tag{4.54}$$

Analogously we obtain for $i > j$,

$$\langle \hat{a}_i^\dagger \hat{a}_j \rangle^{i>j} = \langle \hat{b}_i^\dagger \rangle \prod_{x=j+1}^{i-1} \langle \exp(-i\theta \hat{n}_x) \rangle \langle \exp(-i\theta \hat{n}_j) \hat{b}_j \rangle \\ = \frac{\tilde{C}}{\tilde{z}} \left[ \exp(i\Delta\beta_0) \tilde{z} \right]^{i-j}, \tag{4.55}$$

where the tilde denotes complex conjugation. Thus the full anyonic pair-correlation function, in the Gutzwiller frame, can be written as

$$\langle \hat{a}_i^\dagger \hat{a}_j \rangle = \delta_{ij} n_0 + (1 - \delta_{ij}) \left\{ \frac{\tilde{C}}{\tilde{z}} \left[ \exp(i\Delta\beta_0) \tilde{z} \right]^{i-j} + \frac{C}{z} \left[ \frac{\exp(i\Delta\beta_0)}{z} \right]^{i-j} \right\}. \tag{4.56}$$

Here again the pair-correlation function only depends on the difference of the two site indices $i$ and $j$. Now we have to Fourier transform Eq. (4.48) to get the anyonic quasi-momentum distribution

$$\langle \hat{n}_k^a \rangle = \frac{1}{L} \sum_{i,j=1}^{L} \exp\left[ ik(i-j) \right] \langle \hat{a}_i^\dagger \hat{a}_j \rangle. \tag{4.57}$$

In the next step we split the sum according to Q (4.48)–(4.50)

$$\langle \hat{n}_k^a \rangle = n_0 + \frac{1}{L}\sum_{i<j} \exp\left[ik(i-j)\right] \langle \hat{a}_i^\dagger \hat{a}_j \rangle^{i<j} + \frac{1}{L}\sum_{i>j}^{L} \exp\left[ik(i-j)\right] \langle \hat{a}_i^\dagger \hat{a}_j \rangle^{i>j}$$
$$= n_0 + \frac{1}{L}\sum_{i<j} \exp\left[ik(i-j)\right] \frac{C}{z}\left[\frac{\exp(i\Delta\beta_0)}{z}\right]^{i-j} + \frac{1}{L}\sum_{i>j} \exp\left[ik(i-j)\right] \frac{\tilde{C}}{\tilde{z}}\left[\exp(i\Delta\beta_0)\tilde{z}\right]^{i-j}. \tag{4.58}$$

Now Eq. (4.58) can be calculated by using the property of the geometric sum $\sum_{i=a}^{b} q^i = \frac{q^a - q^{b-1}}{1-q}$ with $a, b \in \mathbb{N}$.
After a rather lengthy but straight-forward calculation, the quasi-momentum distributions of anyons is given by

$$\langle \hat{n}_k^a \rangle = n_0 + \frac{|C|}{L}\left( \frac{\exp\left\{i\left[k + \Delta\beta_0 - \mathrm{Arg(C)}\right]\right\} - \frac{\exp\{i[\mathrm{Arg(z)}-\mathrm{Arg(C)}]\}(|z|\exp\{i[k+\Delta\beta_0-\mathrm{Arg(z)}]\})^L}{|z|}}{2 - \left(|z|\exp\left\{i\left[k + \Delta\beta_0 - \mathrm{Arg(z)}\right]\right\}\right) + \frac{\exp\{-i[k+\Delta\beta_0-\mathrm{Arg(z)}]\}}{|z|}} + \mathrm{c.c.} \right)$$

$$- \frac{2(L-1)|C|}{L}\left( \frac{|z|\cos\left[\mathrm{Arg(C)} - \mathrm{Arg(z)}\right] - \cos\left[k + \Delta\beta_0 - \mathrm{Arg(C)}\right]}{|z|^2 - 2|z|\cos\left[k + \Delta\beta_0 - \mathrm{Arg(C)}\right] + 1} \right), \tag{4.59}$$

where we have used the polar decompositions $C = |C|\exp\left[i\mathrm{Arg(C)}\right]$ and $z = |z|\exp\left[i\mathrm{Arg(z)}\right]$. In order to evaluate the thermodynamic limit, the following relations are crucial

$$\sup_{\theta \neq 0} |z| = 1, \tag{4.60}$$

$$\max\left|\exp\left\{i\left[k + \Delta\beta_0 - \mathrm{Arg(z)}\right]\right\}\right| = 1. \tag{4.61}$$

Out of (4.52) and (4.53) it follows that $\sup_{\theta\neq 0}\left|\left(|z|\exp\left\{i\left[k + \Delta\beta_0 - \mathrm{Arg(z)}\right]\right\}\right)\right| = 1$ and thus, $\lim_{L\to\infty} \frac{(|z\exp\{i[k+\Delta\beta_0-\mathrm{Arg(z)}]\})L}{L} \longrightarrow 0$.
Thus the anyonic quasi-momentum distribution in the thermodynamic limit is given by

$$\langle \hat{n}_k^a \rangle_{L\to\infty} = n_0 + -2|C|\left\{ \frac{|z|\cos\left[\mathrm{Arg(C)} - \mathrm{Arg(z)}\right] - \cos\left[k + \Delta\beta_0 - \mathrm{Arg(C)}\right]}{|z|^2 - 2|z|\cos\left[k + \Delta\beta_0 - \mathrm{Arg(C)}\right] + 1} \right\}. \tag{4.62}$$

In the following, the quasimomentum-distribution for anyons is shown for different values of the statistical parameter and different densities ((FIG. 4.11)). As in the bosonic case the peak of the quasi-momentum distribution is shifted, but to positive momenta, this is due the non-local string operator attached to the bosonic operators [2], i.e. the Jordan-Wigner anyons condense roughly at $k \approx -\theta + \mathrm{Arg}(C)$. In (FIG. 4.11 a) the distribution is shown for low densities.
The peak which is narrow for small values of $\theta$ is getting broader as $\theta$ increases. We interpret this as the subtle transmutation from a boson-like distribution to a kind of Fermi-edge. This effect seems to progress for higher densities (FIG. 4.11 b). Nevertheless, in (FIG. 4.11 c) the effect seems to dim for $n_0 > 1$, in exchange to an enlarged background distribution. Especially for $\theta = \pi$, the background is close to $\langle \hat{n}_k^a \rangle \approx 1$ and thus the broad peak on top can be interpreted as an occupation above the Fermi-edge due to the pseudo-fermionic character of the anyons. Similar to the bosonic case, $\theta = \frac{\pi}{2}$ seems to be a special point, where the momentum shift seems to diminish.

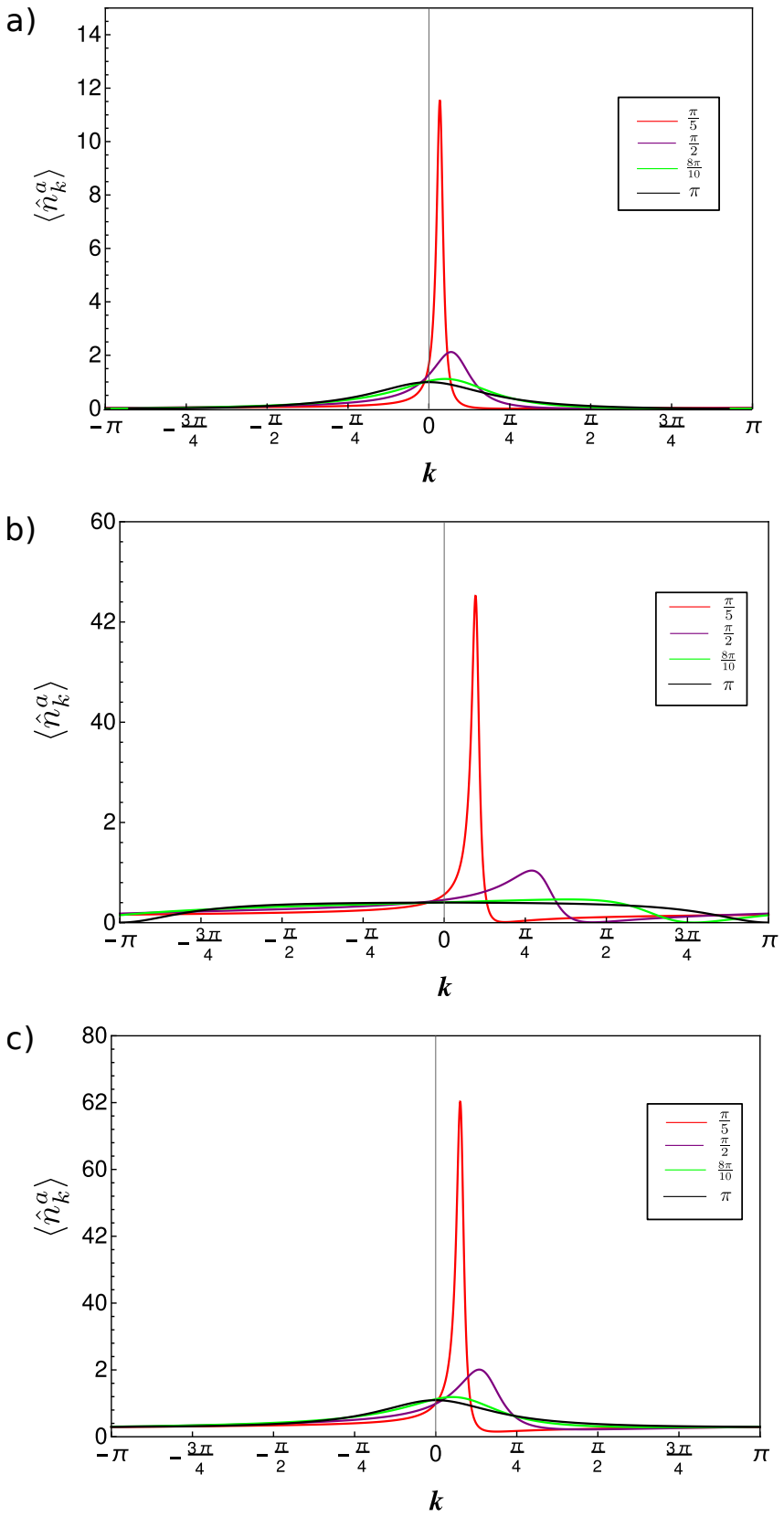


**FIG. 4.11:** Anyonic quasi-momentum distribution $\langle \hat{n}_k^a \rangle$ for densities a) $n_0 = 0.25$, b) $n_0 = 0.75$, c) $n_0 = 1.25$, and $\frac{U}{J} = 10$, system length $L = 100$ and different values of $\theta$.

# 5 Mean-Field Decoupling

In the last chapter of this thesis, we propose a mean-field decoupling scheme in the spirit of our modified Gutzwiller ansatz (4.7). This mean-field ansatz is used to decouple the bi-local product of creation and annihilation operators of the hopping term in (4.13), resulting in a purely local Hamiltonian. The basic idea is to substitute the creation and annihilation operators in the hopping term by their expectation values and the fluctuation around them

$$\hat{a}_i \longrightarrow \langle \hat{a}_i \rangle + \delta\hat{a}_i, \tag{5.1}$$

where only the fluctuations $\delta\hat{a}_i$ have an operator character. Subsequently one neglects all resulting terms which are at least quadratic in the fluctuations $\delta\hat{a}_i^2 \approx 0$.
In preparation of the decoupling scheme we introduce a slight change of notation by collecting all operators acting at site $j$ to one single operator $\hat{c}_j^\dagger = \hat{b}_j^\dagger \exp(i\theta\hat{n}_j)$ [1]. Additionally we use the bi-partite structure of the one-dimensional lattice and distinguish between even and odd sites. Thus the Hamiltonian (4.13) can be written as

$$\hat{H} = \frac{U}{2}\sum_{j=1}^{L}\hat{n}_j\left(\hat{n}_j - 1\right) - J\sum_{j=1}^{\frac{L}{2}}\left[\hat{c}_{2j-1}^\dagger\hat{b}_{2j} + \hat{c}_{2j}^\dagger\hat{b}_{2j+1} + \text{h.c.}\right] - \mu\sum_{j=1}^{L}\hat{n}_j. \tag{5.2}$$

Furthermore any spatial dependence of the decoupled operators is usually neglected in the mean-field scheme as long as homogeneity is ensured. Nevertheless this assumption might be too restrictive in order to account for non-uniform phases [26]. To overcome this fact we decompose the expectation value in every partition in absolute value and a position-dependent phase

$$\langle \hat{b}_{2j} \rangle = \alpha_1^{2j} = \text{Abs}(\alpha_1)\exp(i2j\nu_e), \tag{5.3}$$
$$\langle \hat{c}_{2j} \rangle = \alpha_2^{2j} = \text{Abs}(\alpha_2)\exp(i2j\eta_e), \tag{5.4}$$
$$\langle \hat{b}_{2j+1} \rangle = \alpha_1^{2j+1} = \text{Abs}(\alpha_1)\exp\left[i(2j+1)\nu_o\right], \tag{5.5}$$
$$\langle \hat{c}_{2j+1} \rangle = \alpha_2^{2j+1} = \text{Abs}(\alpha_2)\exp\left[i(2j+1)\eta_o\right], \tag{5.6}$$

as in our modified Gutzwiller ansatz (4.7), where the subscripts of the phases denote odd and even sites, respectively. The Eqs. (5.3)–(5.6) are the self-consistency relations of the mean-field, where the RHSs denote the variational parameters which extremize the Hamiltonian in that state, with respect to whom the expectation value of the LHSs is built. Now the bi-local terms in (5.2) can be decoupled according to

$$\begin{aligned}
\hat{c}_{2j-1}^\dagger\hat{b}_{2j} &\approx -\left(\alpha_2^{2j-1}\right)^*\alpha_1^{2j} + \left(\alpha_2^{2j-1}\right)^*\hat{b}_{2j} + \alpha_1^{2j}\hat{c}_{2j-1} \\
\hat{c}_{2j}^\dagger\hat{b}_{2j+1} &\approx -\left(\alpha_2^{2j}\right)^*\alpha_1^{2j+1} + \left(\alpha_2^{2j}\right)^*\hat{b}_{2j+1} + \alpha_1^{2j+1}\hat{c}_{2j}
\end{aligned} \tag{5.7}$$

which leads to the following mean-field Hamiltonian

$$\begin{aligned}\hat{H}_{\mathrm{MF}} =& \frac{U}{2}\sum_{j=1}^{L}\hat{n}_j\left(\hat{n}_j-1\right)-\mu\sum_{j=1}^{L}\hat{n}_j-J\sum_{j=1}^{\frac{L}{2}}\left[B_o^*\left(\eta_o,\nu_e,\hat{n}_{2j}\right)\hat{b}_{2j}+A_e^*\left(\eta_e,\nu_o,\hat{n}_{2j+1}\right)\hat{b}_{2j+1}+\mathrm{h.c.}\right]\\ &+2J\mathrm{Abs}(\alpha_1)\mathrm{Abs}(\alpha_2)\sum_{j=1}^{\frac{L}{2}}\left\{\cos\left[2j(\eta_o-\nu_e)-\eta_o\right]+\cos\left[2j(\eta_e-\nu_o)-\eta_e\right]\right\}.\end{aligned} \tag{5.8}$$

Note that we have re-inserted the expression for $\hat{c}_j^\dagger=\hat{b}_j^\dagger\exp(i\theta\hat{n}_j)$ again. The prefactors in the hopping term of (5.8), $B_o^*$ and $A_e^*$, are given by

$$A_e^*\left(\eta_e,\nu_o,\hat{n}_{2j+1}\right)=\left\{\mathrm{Abs}(\alpha_2)\exp\left(-i2j\eta_e\right)+\mathrm{Abs}(\alpha_1)\exp\left[-i(2j+2)\nu_o\right]\exp\left(-i\theta\hat{n}_{2j+1}\right)\right\}, \tag{5.9}$$

$$B_o^*\left(\eta_o,\nu_e,\hat{n}_{2j}\right)=\left\{\mathrm{Abs}(\alpha_2)\exp\left[-i(2j-1)\eta_o\right]+\mathrm{Abs}(\alpha_1)\exp\left[-i(2j+1)\nu_e\right]\exp\left(-i\theta\hat{n}_{2j}\right)\right\}. \tag{5.10}$$

In order to obtain the quantum phase diagram one usually identifies the norm of the expectation value $\alpha_j$ with the order parameter of the system, which distinguishs between the two phases, i.e. it is zero in one phase while having a finite value in the other. In the case of the superfluid to Mott insulator transition, one identifies $\mathrm{Abs}(\alpha_\mathrm{j})^2$ with the condensate density, which is non-zero in the superfluid phase and zero in the Mott state.
The self-consistency relations (5.3)–(5.6) define a map, which can be linearized around the trivial solution $\alpha_j\approx 0$. In that case the hopping term can be treated perturbatively, and the ground-state in the lowest non-trivial order is given by $|\,\Psi\,\rangle\approx|\,n\,\rangle+|\,\Psi_1\,\rangle$. Here $|\,\Psi_1\,\rangle$ can be obtained by a first-order Rayleigh-Schrödinger perturbation theory

$$\begin{aligned}|\,\Psi_1\,\rangle =& \sum_{n\neq n'}\frac{\langle\,n'\,|\hat{H}_{\mathrm{pert}}|\,n\,\rangle}{E_n^0-E_{n'}^0}|\,n'\,\rangle\\ =&J\left[\frac{\sqrt{n}}{E_n^0-E_{n-1}^0}A_e^*\left(\eta_e,\nu_o,n-1\right)|\,n-1\,\rangle_{2j+1}+B_o^*\left(\eta_o,\nu_e,n-1\right)|\,n-1\,\rangle_{2j}\right]\\ &+J\left[\frac{\sqrt{n+1}}{E_n^0-E_{n+1}^0}A_e\left(\eta_e,\nu_o,n\right)|\,n+1\,\rangle_{2j+1}+B_o\left(\eta_o,\nu_e,n\right)|\,n+1\,\rangle_{2j}\right],\end{aligned} \tag{5.11}$$

where $|\,n\,\rangle=C\prod_{i=1}^{L}(\hat{b}_i^\dagger)^n\mid 0\rangle_i$ and $E_n^0|\,n\,\rangle=\hat{H}_0|\,n\,\rangle$ are the un-perturbed eigenstates and eigenvalues respectively. The self-consistency equations (5.3)–(5.6) can be evaluated according to

$$\mathrm{Abs}(\alpha_1)\exp(i2j\nu_e)=\langle\,\Psi_1\,|\hat{b}_{2j}|\,n\,\rangle+\langle\,n\,|\hat{b}_{2j}|\,\Psi_1\,\rangle, \tag{5.12}$$

$$\mathrm{Abs}(\alpha_2)\exp(i2j\eta_e)=\langle\,\Psi_1\,|\hat{c}_{2j}|\,n\,\rangle+\langle\,n\,|\hat{c}_{2j}|\,\Psi_1\,\rangle, \tag{5.13}$$

$$\mathrm{Abs}(\alpha_1)\exp\left[i(2j+1)\nu_o\right]=\langle\,\Psi_1\,|\hat{b}_{2j+1}|\,n\,\rangle+\langle\,n\,|\hat{b}_{2j+1}|\,\Psi_1\,\rangle, \tag{5.14}$$

$$\mathrm{Abs}(\alpha_2)\exp\left[i(2j+1)\eta_o\right]=\langle\,\Psi_1\,|\hat{c}_{2j+1}|\,n\,\rangle+\langle\,n\,|\hat{c}_{2j+1}|\,\Psi_1\,\rangle. \tag{5.15}$$

Additionally we demand for consistency reasons that the absolute values of the variational

parameters coincide for both lattice partitions and depend not on the lattice position $j$

$$\begin{aligned}\exp(-i2j\nu_e)\left[\langle\,\Psi_1\,|\hat{b}_{2j}|\,n\,\rangle+\langle\,n\,|\hat{b}_{2j}|\,\Psi_1\,\rangle\right]&=\exp\left[-i(2j+1)\nu_o\right]\left[\langle\,\Psi_1\,|\hat{b}_{2j+1}|\,n\,\rangle+\langle\,n\,|\hat{b}_{2j+1}|\,\Psi_1\,\rangle\right],\\ \exp(-i2j\eta_e)\left[\langle\,\Psi_1\,|\hat{c}_{2j}|\,n\,\rangle+\langle\,n\,|\hat{c}_{2j}|\,\Psi_1\,\rangle\right]&=\exp\left[-i(2j+1)\eta_o\right]\left[\langle\,\Psi_1\,|\hat{c}_{2j+1}|\,n\,\rangle+\langle\,n\,|\hat{c}_{2j+1}|\,\Psi_1\,\rangle\right].\end{aligned} \tag{5.16}$$

Out of (5.16) the phases for the variational parameters are already fixed to the specific values

$$\eta_e = \pi n_2, \tag{5.17}$$
$$\eta_o = \pi(n_2 - n_1), \tag{5.18}$$
$$\nu_e = 2\pi n_2, \tag{5.19}$$
$$\nu_o = \pi(n_2 + n_1) \quad \text{with} \quad n_1, n_2 \in \mathbb{Z}. \tag{5.20}$$

After a lengthy but straight-forward calculation the Eqs. (5.12)–(5.15) finally reduce to

$$\begin{pmatrix}\mathrm{Abs}(\alpha_1)\\ \\ \mathrm{Abs}(\alpha_2)\end{pmatrix} = J\begin{bmatrix}C\,(\theta,n) & (-1)^{n_2-n_1}D\,(n)\\ \\ D\,(n) & (-1)^{n_2+n_1}C^*\,(\theta,n)\end{bmatrix}\begin{pmatrix}\mathrm{Abs}(\alpha_1)\\ \\ \mathrm{Abs}(\alpha_2)\end{pmatrix} \tag{5.21}$$

with the following abbreviations

$$C\,(\theta,n) = \frac{n\exp\left[i\theta(n-1)\right]}{E_n^0 - E_{n-1}^0} + \frac{(n+1)\exp\left[i\theta n\right]}{E_n^0 - E_{n+1}^0}, \tag{5.22}$$

$$D\,(n) = \frac{n}{E_n^0 - E_{n-1}^0} + \frac{(n+1)}{E_n^0 - E_{n+1}^0}. \tag{5.23}$$

The corresponding eigenvalues of the self-consistency map are given by

$$\begin{aligned}\frac{\lambda_\pm}{J} =& \frac{C\,(\theta,n) + (-1)^{n_2+n_1}C^*\,(\theta,n)}{2} \\ &\pm\sqrt{\frac{\left[C\,(\theta,n) + (-1)^{n_2+n_1}C^*\,(\theta,n)\right]^2}{4} - \left[(-1)^{n_2+n_1}\mathrm{Abs}\left[C\,(\theta,n)\right]^2 - (-1)^{n_2-n_1}D\,(n)^2\right]}.\end{aligned} \tag{5.24}$$

As the self-consistency relations are solved in an iterative manner, the onset of unstable solutions is given by the condition $\max\left[\mathrm{Re}\,(\lambda_\pm)\right] = 1$. This yields the critical coupling $J_{\mathrm{crit}}$ where the rise of the instability towards the superfluid region in the phase diagram occurs.
Until now we have not fixed the additional phases of the variational parameters $n_i$ yet, as the corresponding extremalization procedure has not been finished in this thesis. Nevertheless, there remain only two possibilities for the corresponding phase diagram as the integers $n_i$ occur either as a sum or difference in (5.24). If they are chosen to be both either even or odd, we reproduce the phase diagram of Ref. [1], but if they are chosen such that they differ in their parity we obtain a slightly different one. In order to further interpret this we re-insert (5.17)–(5.20) in (5.3)–(5.6), which leads to

$$\langle\hat{b}_{2j}\rangle = \mathrm{Abs}(\alpha_1), \tag{5.25}$$
$$\langle\hat{c}_{2j}\rangle = \mathrm{Abs}(\alpha_2), \tag{5.26}$$
$$\langle\hat{b}_{2j+1}\rangle = \mathrm{Abs}(\alpha_1)(-1)^{n_2-n_1}, \tag{5.27}$$
$$\langle\hat{c}_{2j+1}\rangle = \mathrm{Abs}(\alpha_2)(-1)^{n_2+n_1}. \tag{5.28}$$

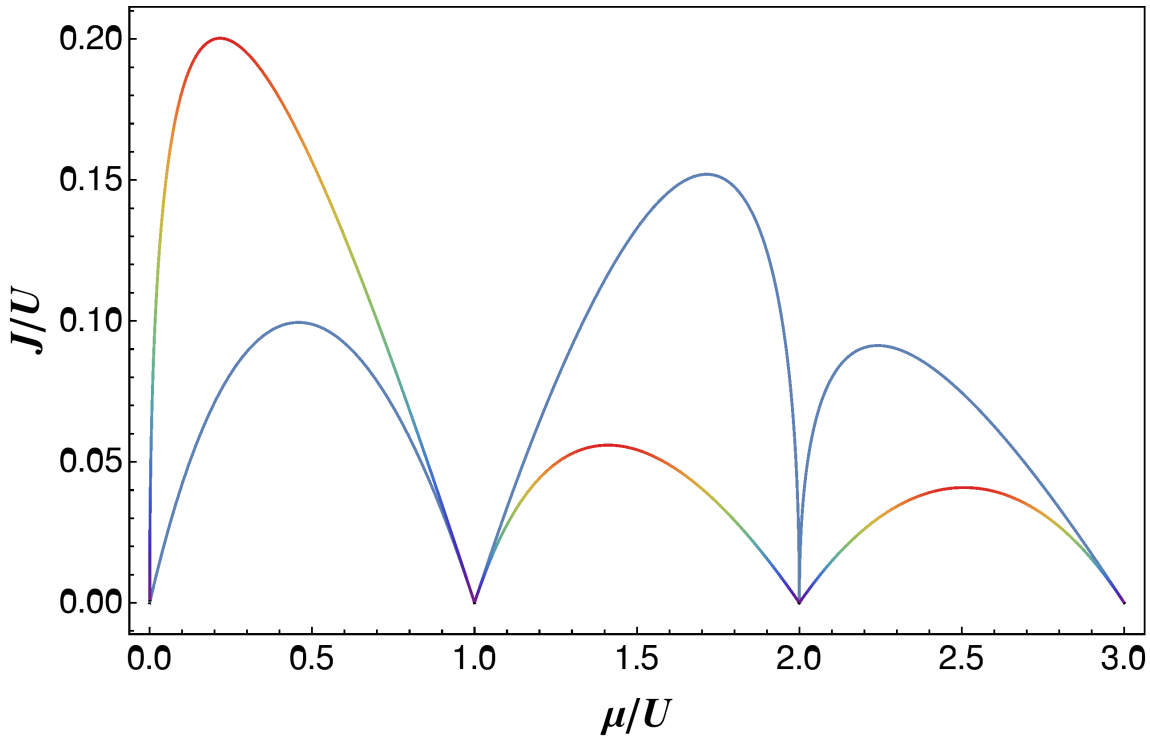


**FIG. 5.1:** Quantum phase-diagram of the mean-field Hamiltonian (5.8) for $\theta = \frac{\pi}{4}$. The blue line is equivalent to the one in Ref. [1] corresponding to the case where both integers in (5.27)–(5.28) are either both odd or even. The colored curve corresponds to the case where one of the integers is odd and the other one even.

If now both integers are even or odd respectively, then the expectation values are equal on both lattice partitions, i.e. $\langle \hat{b}_{2j} \rangle = \langle \hat{b}_{2j+1} \rangle$ and $\langle \hat{c}_{2j} \rangle = \langle \hat{c}_{2j+1} \rangle$, denoted by the blue curves in Fig. 5.1–Fig. 5.3. On the other hand if one of the phases is odd and the other is even, we obtain $\langle \hat{b}_{2j} \rangle = -\langle \hat{b}_{2j+1} \rangle$ and $\langle \hat{c}_{2j} \rangle = -\langle \hat{c}_{2j+1} \rangle$ which is denoted by the colored curves in Fig. 5.1–Fig. 5.3. In the latter case the corresponding phase is called broken-symmetry superfluid [26], which arises naturally in our ansatz. Thus it still has to be shown, by a minimization of the corresponding energy, which of both possibilities is realized at a given point in the phase-diagram. With this our decoupling ansatz is, in principle, capable of describing both transitions, i.e. either from Mott to superfluid or from Mott to broken-symmetry superfluid, in contrast to Ref. [1].

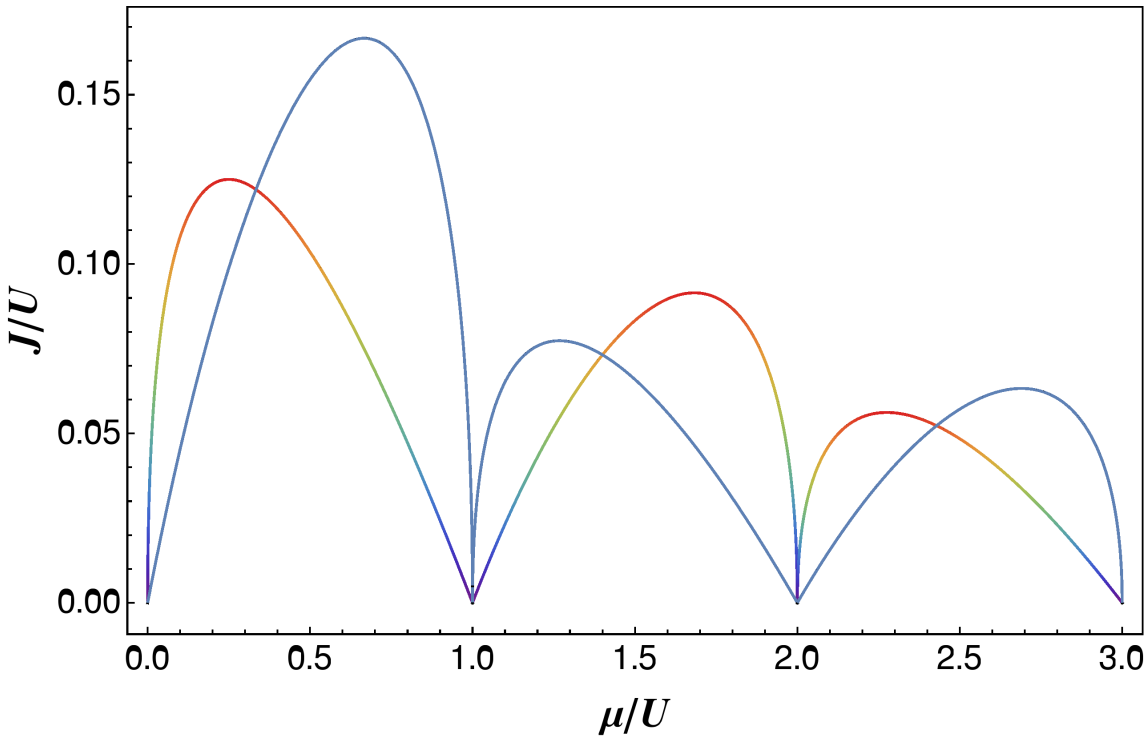


**FIG. 5.2:** Quantum phase-diagram of the mean-field Hamiltonian (5.8) for $\theta = \frac{\pi}{2}$. Plot legend as in Fig. 5.1

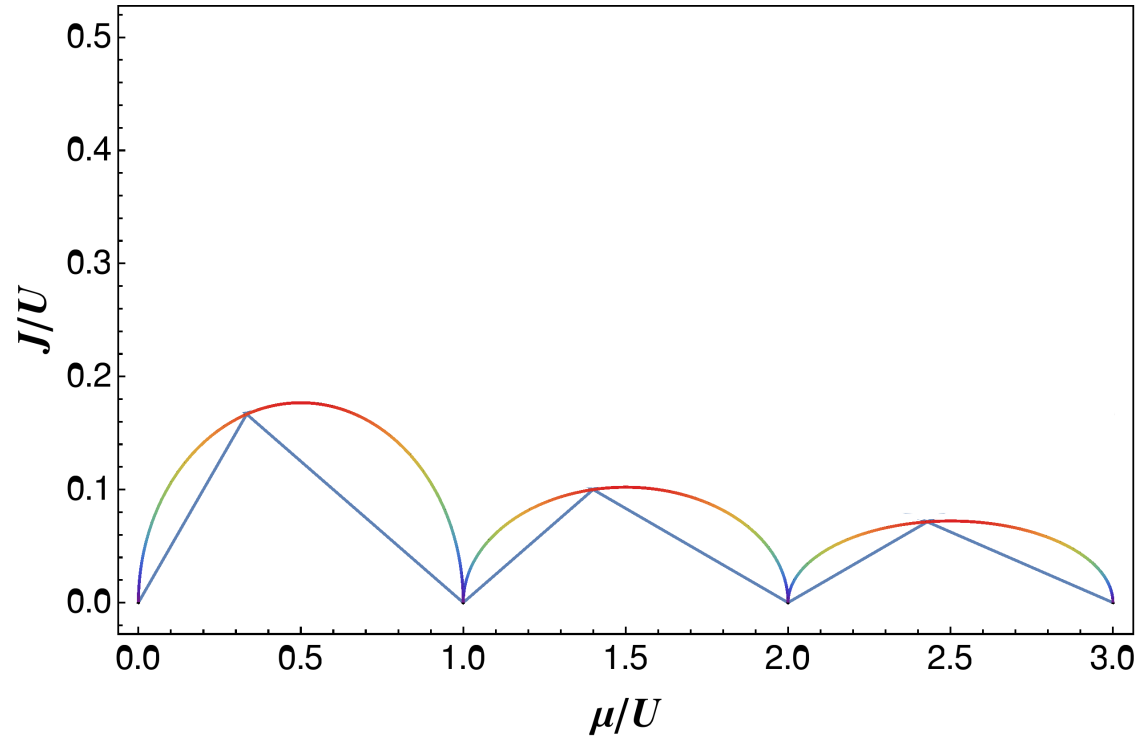


**FIG. 5.3:** Quantum phase-diagram of the mean-field Hamiltonian (5.8) for $\theta = \pi$. Plot legend as in Fig. 5.1

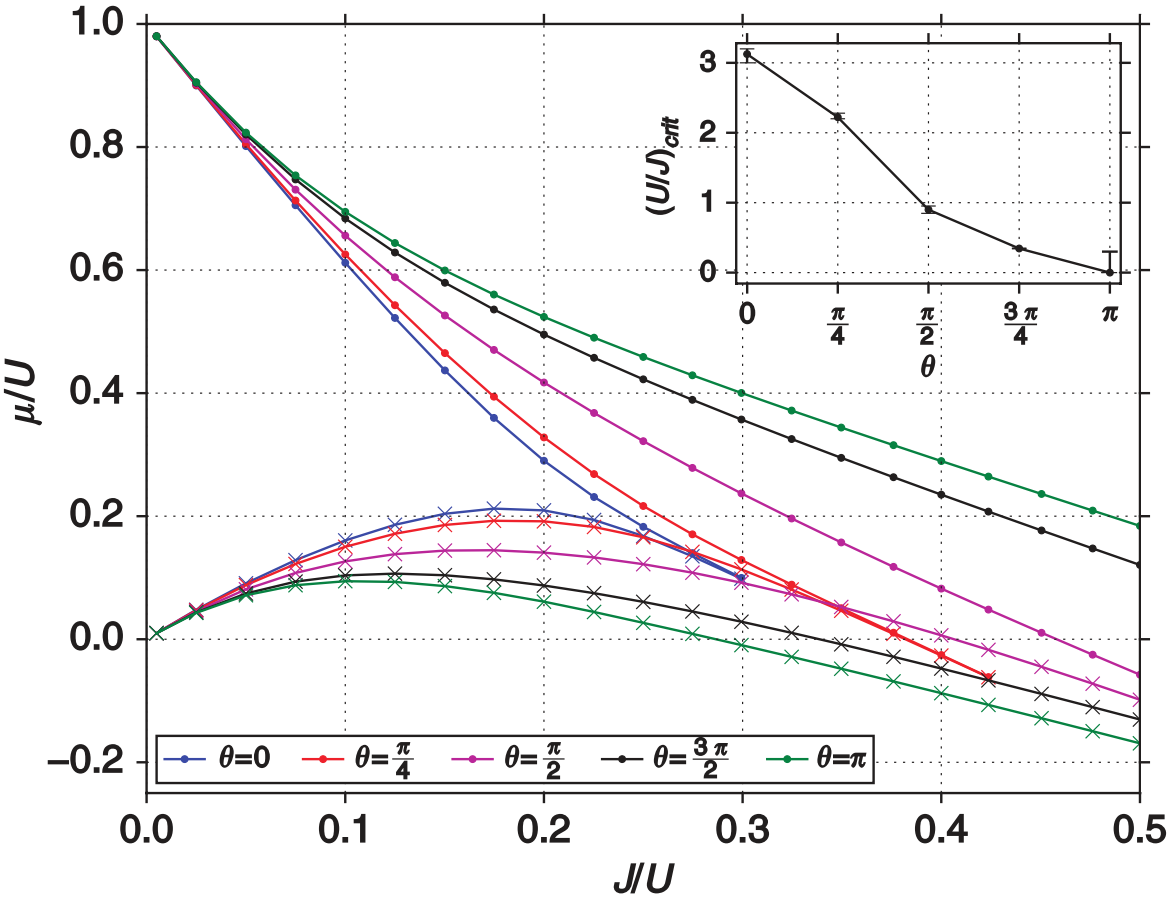


**FIG. 5.4:** Quantum phase diagram obtained in Ref. [1] via DMRG for different statistical parameters. The inlet shows how the tip of the BKT transition decreases with increasing $\theta$

In Fig. 5.1 to Fig. 5.3 the impact of a non-zero statistical parameter on the phase boundary between Mott insulator and superfluid can be observed. The presence of the correlated hopping term in (4.13) seems to lead to a deformation of the Mott plateaus. As already discussed in Ref. [1], the insulating region in the phase-diagram seems to grow when the pseudo-fermionic limit is approached. This can be interpreted again as an effective interaction induced by the progressing anti-symmetrization of the non-local commutators. Furthermore if one compares the mean-field results with the DMRG data, then it turns out, that for some values of the statistical parameter $\theta$ our new solution of the phase curve is closer to the quasi-exact solutions, for example Fig. 5.1. Additionally in Fig. 5.4 it can be seen that the Berezinsky–Kosterlitz–Thouless(BKT)-like transition is bent to the $\frac{J}{U}$-axis, whereas the mean-field approach of Ref. [1] is bent in the other direction. Of course these observations have still to be verified with a corresponding minimization procedure.

# 6 Conclusion

At the end of this thesis we would like to subsume the most crucial points. First of all, the notion of one-dimensional anyons was enlighted by observing that the deformed commutation relations (2.2) do not originate from the topological properties of the one-dimensional configuration space, in contrast to their two-dimensional counterpart. The reason why they can be consistently defined in one dimension is the natural linear order on such spaces where commutation relations such as (2.2) can be introduced a priori.
Additionally as the Anyon-Hubbard model can be mapped to an experimentally feasible bosonic model with density-dependent Peierls phase, the occurrence of one-dimensional anyons is not merely a mathematical curiosity, but physical reality. Also a close inspection of the algebraic structure of the Jordan-Wigner anyons helped to understand that exchange statistics and exclusion behavior are two independent concepts, and thus the claim that anyons transmute from bosons to fermions or vice versa is only partially true. A better notion would be that the Jordan-Wigner anyons transmute from a bosonic exchange statistics to a fermionic one, while preserving the dimension of the local Hilbert space and with that the exclusion behavior.
Of interest is also the symmetry breaking that is induced by the commutation relations (2.2). While the breaking of parity and time-reversal symmetry is more or less obvious on the level of commutators, the loss of translational symmetry, even if periodic boundary conditions for the Anyon-Hubbard model are assumed, is far from being trivial and is usually neglected in the literature. Additionally the appearance of anti-periodic or periodic boundary conditions for even or odd particle number in the limit $\theta \longrightarrow \pi$ shows the rise of fermionic behavior in a remarkable manner. A consequence of neglecting the boundary term is that the Anyon-Hubbard model with periodic boundary conditions is not unitarily equivalent to (4.13), i.e. (4.13) would be unitarily equivalent to an Anyon-Hubbard model with twisted boundary conditions which explicitly depend on the statistical parameter $\theta$. Furthermore the symmetry analysis of chapter 3 showed for some particular values of $\theta$ that there can be situations where the bosonic version of the Anyon-Hubbard model breaks two discrete symmetries separately but is invariant with respect to the combined action, which also remains unrecognized in the literature to our knowledge.
The Gutzwiller ansatz that was worked out in chapter 4 is capable of describing qualitatively the rise of energy when $\theta$ approaches the pseudo-fermionic limit according to Fig. 4.2, in agreement with the DMRG data Fig. 4.3 and in opposition to Ref. [2]. This rise can be interpreted as an effective interaction [39], which is induced by the anti-symmetrization of the non-local commutation relation. This is interesting by itself, as the intrinsic repulsive interaction of fermions, namely the Pauli blockade, is caused by the local anti-commutators. Additionally, despite the questionable validity of mean-field calculations in low-dimensional systems, the signatures of the broken parity or time-reversal symmetry could be resolved by the shifted bosonic quasi-momentum distributions according to Fig. 4.5, Fig. 4.8, Fig. 4.9. In particular the obtained distributions are in better agreement with the high-precision data of the DMRG-calculations [38] (Fig. 4.6, Fig. 4.7, Fig. 4.10), than Ref. [2]. Furthermore, even if it might be a purely academic exercise, the quasi-momentum distribution of the Jordan-Wigner anyons are also obtained

by the modified Gutzwiller ansatz. With them a transmutation from a bosonic condensate to a kind of smoothed out Fermi-edge could be observed Fig. 4.11. In the last chapter of this thesis we proposed a mean-field decoupling scheme in order to calculate the quantum phase diagram of the Anyon-Hubbard model, and with that generalized the results of Ref. [1]. The phase border we have obtained seems to agree better with the DMRG-data for some values of the statistical parameter, where it should be noted, that the whole extremalization process could not be finished during the time of the thesis. Nevertheless our mean-field ansatz naturally includes the so called broken-symmetry superfluid phase, arising out of simple consistency considerations, see Ref. [26]

# 7 Outlook

As the diploma thesis is now at the end, as time is always a limiting factor, we would like to list a few things that would be interesting to study in order to further understand the properties of interacting one-dimensional anyons in optical lattices. First of all their presence is still speculative as the various theoretical proposals for their experimental realization have not yet been implemented. Additionally the quasi-momentum distributions of anyons might not even be a measurable quantity. Therefore, it would be desirable to have access to quantities, which are invariant with respect to the Jordan-Wigner transformation in order to verify the presence of anyons. An illustrative example is provided by the density distribution for open boundary conditions, i.e. Friedel oscillations [23]. As Friedel oscillations are a typical fermionic feature and are not observed in bosonic systems, their appearance in the bosonic model with correlated hopping would be a direct proof of the transmutation from a bosonic to a fermionic exchange statistics. Furthermore, the impact of finite temperature and the dynamics have not been investigated for the soft-core case, although these topics have been studied preliminarily for the hard-core case [40] [41], where the phase in the correlated hopping term vanishes anyway.
Another point is that the Jordan-Wigner transformation can also be applied to fermions as discussed in chapter 2. Such an anyon to fermion mapping would not lead to a correlated hopping term for a given anyonic Hamiltonian, for the same reason as in the hard-core boson case. Nevertheless the correlation functions of such a system might show some highly non-trivial features due to their anyonic origin. Furthermore a different anyonic Hamiltonian should be considered for the fermionic case, as the Anyon-Hubbard model (2.1) kind of incorporates already a bosonic description due to the form of the interaction term.
As seen in chapter 3 there might be different discrete symmetries with respect to whom the bosonic model (4.13) is invariant. The behavior of systems with respect to these discrete space-time symmetries is usually used to distinguish different topological states of matter in the interaction-free case. A similar rigorous procedure to classify the Anyon-Hubbard model would be highly desirable. Delicate here is that even in the case of a vanishing on-site interaction the system is still intrinsically interacting due to the correlated hopping term.

# 8 Acknowledgement

First of all I want to thank Prof. Dr. Sebastian Eggert sincerely for offering me the possibility to do my diploma thesis in his working group. Furthermore I want to thank Prof. Dr. Micheal Fleischhauer for being the second reviewer of this thesis. Primarily I would like to show my gratitude to Priv. Doz. Dr. Axel Pelster for all his unrestricted support during the accomplishment of my thesis and the time before. For the numerous discussions, that he is always willing to share his knowledge and encouraging me through the whole working period. Furthermore I would like to thank Prof. Dr. Antun Balaž and his working group at the Scientific Computing Laboratory, Institute of Physics Belgrade for the kind hospitality during my research visit in Serbia. I also want to thank Prof Dr. Francisco Ednilson Alves dos Santos from the universidade federal de Sao Carlos in Brazil for supporting me during my stay in Brazil. Additionally I want to thank the whole working group and especially Denis Morath, Dominik Straßel and Kevin Jägering for invaluable discussions about physics in general and all the assistance they offered to me unselfishly during my time in the working group. Special thanks are devoted to my colleagues Merten Grupe, Martin Kübler and Kai Kuthan for various support during my studies and relaxing coffee breaks. I also want to thank all my friends for being there anytime and my parents for supporting me.
Last but most importantly I want to express my deepest gratitude to Magda and Liselotte, as without their love and support from day one, I would not be here. Thank you for all.

Name: Martin Bonkhoff Datum: 1. 12. 2016

Erklärung gem. § 16 Abs. 7 Diplomsprüfungsordnung (DPO) Biophysik

Die Diplomarbeit mit dem Thema
Interacting Anyons In A One Dimensional Optical Lattice
abgegeben am 1. 12. 2016 wurde am 01. 03. 2016
von Herrn Prof. Dr. Sebastian Eggert an mich ausgegeben und betreut.

Ich versichere, dass ich die Arbeit selbstständig verfasst und keine anderen als die angegebenen Quellen und Hilfsmittel benutzt habe.

Zum zweiten Gutachter gem. § 17 Abs. 2 DPO bitte ich
Herrn Prof. Dr. Michael Fleischhauer zu bestimmen.

Unterschrift:

# Bibliography


[1] T. Keilmann, S. Lanzmich, I. McCulloch, and M. Roncaglia, "Statistically induced phase transitions and anyons in 1d optical lattices," *Nat. Commun.*, vol. 2, p. 361, 2011.

[2] G. Tang, S. Eggert, and A. Pelster, "Ground-state properties of anyons in a one-dimensional lattice," *New J. Phys.*, vol. 17, no. 12, p. 123016, 2015.

[3] W. Pauli, "The connection between spin and statistics," *Phys. Rev.*, vol. 58, pp. 716–722, 1940.

[4] F. Wilczek, "Quantum mechanics of fractional-spin particles," *Phys. Rev. Lett.*, vol. 49, pp. 957–959, 1982.

[5] A. Khare, *Fractional Statistics and Quantum Theory.* World Scientific Pub Co Inc, second edition ed., 2005.

[6] A. Stern, "Anyons and the quantum Hall effect - A pedagogical review," *Ann. Phys.*, vol. 323, no. 1, pp. 204 – 249, 2008.

[7] B. Paredes, P. Fedichev, J. I. Cirac, and P. Zoller, "$\frac{1}{2}$-anyons in small atomic Bose-Einstein condensates," *Phys. Rev. Lett.*, vol. 87, p. 010402, 2001.

[8] M. Aguado, G. K. Brennen, F. Verstraete, and J. I. Cirac, "Creation, manipulation, and detection of abelian and non-abelian anyons in optical lattices," *Phys. Rev. Lett.*, vol. 101, no. 26, 2008.

[9] G. Feng, G. Long, and R. Laflamme, "Experimental simulation of anyonic fractional statistics with an NMR quantum-information processor," *Phys. Rev. A*, vol. 88, p. 022305, 2013.

[10] J. Leinaas, J. M.and Myrheim, "On the theory of identical particles," *Il Nuovo Cimento B*, vol. 37, no. 1, pp. 1–23, 1977.

[11] C. Beenakker and L. Kouwenhoven, "A road to reality with topological superconductors," *Nat. Phys.*, vol. 12, no. 7, pp. 618–621, 2016.

[12] H. L. Partner, R. Nigmatullin, T. Burgermeister, J. Keller, K. Pyka, M. B. Plenio, A. Retzker, W. H. Zurek, A. del Campo, and T. E. Mehlstäubler, "Structural phase transitions and topological defects in ion Coulomb crystals," *Physica B: Condensed Matter*, vol. 460, pp. 114 – 118, 2015.

[13] A. Kitaev, "Fault-tolerant quantum computation by anyons," *Ann. Phys.*, vol. 303, no. 1, pp. 2 – 30, 2003.

[14] K. Jänich, *Topology (Undergraduate Texts in Mathematics)*. Springer, second correction ed., 1995.

[15] V. Prasolov, *Intuitive Topology (Mathematical World, Vol 4)*. American Mathematical Society, 1995.

[16] E. Fadell and L. Neuwirth, "Configuration spaces," *J. Math.Scand.*, vol. 10, pp. 111–118, 1962.

[17] R. Fox and L. Neuwirth, "The braid groups," *J.Math.Scand.*, vol. 10, pp. 119–126, 1962.

[18] A. Rovenchak, "Fractional statistics: A retrospective view." `http://users.physik.fu-berlin.de/~pelster/Anyon2/rovenchak1.pdf`, 2014. International School and Workshop Anyon Physics of Ultracold Atomic Gases at University of Kaiserslautern.

[19] C. D. Batista and G. Ortiz, "Algebraic approach to interacting quantum systems," *Adv.Phys.*, vol. 53, pp. 1–82, 2004.

[20] F. D. M. Haldane, ""Fractional statistics" in arbitrary dimensions: A generalization of the Pauli principle," *Phys. Rev. Lett.*, vol. 67, pp. 937–940, 1991.

[21] H. S. Green, "A generalized method of field quantization," *Phys. Rev.*, vol. 90, pp. 270–273, 1953.

[22] S. Greschner and L. Santos, "Anyon Hubbard model in one-dimensional optical lattices," *Phys. Rev. Lett.*, vol. 115, p. 053002, 2015.

[23] C. Sträter, S. C. L. Srivastava, and A. Eckardt, "Floquet realization and signatures of one-dimensional anyons in an optical lattice," *Phys. Rev. Lett.*, vol. 117, p. 205303, Nov 2016.

[24] F. H. L. Essler, H. Frahm, F. Göhmann, A. Klümper, and V. E. Korepin, *The one-dimensional Hubbard model*. Cambridge University Press, 2003.

[25] P. H. Seagraves, *Representation of Permutation Operators in Quantum Mechanics*. PhD thesis, University of British Columbia, 1964.

[26] W. Zhang, E. Fan, T. C. Scott, and Y. Zhang, "Beats, broken-symmetry superfluid on a one dimensional Anyon Hubbard model," *arXiv:1511.01712*, 2015.

[27] M. Frau, A. Lerda, and S. Sciuto, "Anyons and deformed lie algebras," *hep-th/9407161*, 1994.

[28] A. Lerda and S. Sciuto, "Anyons and quantum groups," *Nuclear Physics B*, vol. 401, no. 3, pp. 613 – 643, 1993.

[29] P. Jordan and E. Wigner, "Über das Paulische Äquivalenzverbot," *Zeitschrift für Physik*, vol. 47, no. 9, pp. 631–651, 1928.

[30] H. Kleinert, *Gauge Fields in Condensed Matter, Superflow and Vortex Lines*, vol. 1. World Scientific (Singapore), 1989.

[31] H. Kleinert, *Gauge Fields in Condensed Matter, Stresses and Defects*, vol. 2. World Scientific (Singapore), 1989.

[32] D. Jaksch and P. Zoller, "Creation of effective magnetic fields in optical lattices: the Hofstadter butterfly for cold neutral atoms," *New J. Phys.*, vol. 5, no. 1, p. 56, 2003.

[33] F. Trimborn, "Phasenraumdynamik des Bose Hubbard Modells," Master's thesis, University of Kaiserslautern, 2007.

[34] M. Fleischhauer, "Quantum Hall physics and topological states of matter." `http://www.physik.uni-kl.de/agfleischhauer/dokuwiki/doku.php?id=teaching:teaching`, 2016. Lecture notes, University of Kaiserslautern.

[35] B. Damski and J. Zakrzewski, "Mott-insulator phase of the one-dimensional Bose-Hubbard model: A high-order perturbative study," *Phys. Rev. A*, vol. 74, p. 043609, 2006.

[36] M. A. Cazalilla, R. Citro, T. Giamarchi, E. Orignac, and M. Rigol, "One dimensional bosons: From condensed matter systems to ultracold gases," *Rev. Mod. Phys.*, vol. 83, pp. 1405–1466, 2011.

[37] E. Demler, "Strongly correlated systems in atomic and condensed matter physics." `http://cmt.harvard.edu/demler/TEACHING/Physics284/physics284.html`, 2011. lecture notes.

[38] K. Jägering, "Private communications." University of Kaiserslautern, AG Eggert.

[39] S. Greschner, G. Sun, D. Poletti, and L. Santos, "Density-dependent synthetic gauge fields using periodically modulated interactions," *Phys. Rev. Lett.*, vol. 113, p. 215303, Nov 2014.

[40] Y. Hao and Y. Song, "One-dimensional hard-core anyon gas in a harmonic trap at finite temperature," *arXiv:1608.03387*, 2016.

[41] T. M. Wright, M. Rigol, M. J. Davis, and K. V. Kheruntsyan, "Nonequilibrium dynamics of one-dimensional hard-core anyons following a quench: Complete relaxation of one-body observables," *Phys. Rev. Lett.*, vol. 113, p. 050601, 2014.